NUMERICAL ELECTROMAGNETIC MODELING INCLUDING STUDIES OF CHARACTERISTIC DIMENSIONS: A REVIEW

P. KAIKKONEN

Department of Geophysics, University of Oulu, SF-90570 Oulu 57, Finland

Abstract. Recent activity in important approximate methods used in numerical electromagnetic (EM) modeling is reviewed. Comparisons between the results obtained by different numerical methods and between analytical and numerical solutions are presented. The importance of 3D modeling and thin sheet approximations are pointed out.

This review also considers and summarizes studies of characteristic dimensions in three topics: source fields, numerical modeling and physical phenomena in the earth and interpretation. The skin depth (i.e., generally the attenuation) of the EM energy is considered to be the most important and fundamental characteristic dimension.

1. Introduction

The interpretation of electromagnetic (EM) field data is carried out by comparing field and theoretical data with each other. The required theoretical data can be calculated easily only for layered, i.e. one-dimensional (1D) geoelectric structures (e.g., Wait, 1962; Ward, 1967).

Analytical solutions for two-dimensional (2D) structures are difficult to develop, however for the H-polarization case d'Erceville and Kunetz (1962) considered a vertical outcropping fault over either an infinitely resistive or infinitely conductive basement, Rankin (1962) an outcropping dike and Weaver (1963) an infinite vertical fault. Therefore the bulk of more complex 2D theoretical data have been produced with analogue model experiments (e.g., Rankin *et al.*, 1965; Dosso, 1966, 1973) or numerical methods. The usefulness and effectiveness of analogue modeling, e.g., in magnetotelluric (MT) interpretation is distinct and recognized, particularly for three-dimensional (3D) cases (e.g., Nienaber *et al.*, 1979). However, it is well-known that analogue modeling has certain limitations, e.g., material problems, making it difficult to model intermediate conductivity contrasts.

Numerical modeling of 2D or 3D structures can be carried out by the methods in which the techniques of either differential equations (DE) or integral equations (IE) are used. Both procedures result in solving a set of linear algebraic equations. The DE technique results in large, but sparse and banded matrices, because the unknown field quantity used in the formulation has to be solved at every node of a mesh, which covers the whole space. In the IE approach the unknown fields only need to be solved for in anomalous regions which are covered by the mesh. Thus, although the matrices in the IE method are full, their dimensions and respectively the computer storage requirements are smaller than in the DE methods.

Surveys in Geophysics **8** (1986) 301–337.

The first 2D geoelectromagnetic applications of the IE method were presented by Parry (1969) and Hohmann (1971). The IE method, due to its properties mentioned above, is most likely the best numerical method in solving 3D EM problems, provided that the inhomogeneity is not too large and there are only a few of them (Raiche, 1974; Weidelt, 1975; Hohmann, 1975; Lajoie and West, 1976; Ting and Hohmann, 1981; Hvoždara, 1981a, b; Das and Verma, 1981, 1982).

The EM responses of really complex geological structures have to be solved by some DE approach. The finite difference (FD) method was the first one used in numerical MT solutions (Neves, 1957) and since then it has been until recently probably the most popular and most widely used method among the induction community. This popularity is most likely due to the FD program listing published by Jones and Pascoe (1971). Other FD papers are presented, e.g., by Jones and Price (1970), Jones (1974), Brewitt-Taylor and Weaver (1976), Praus (1976), Jones and Vozoff (1978), Zhdanov *et al.* (1982).

The transmission surface analogy is closely related to the FD method and has also been used in solving geoelectromagnetic problems (e.g., Madden and Thompson, 1965; Swift, 1971; Ku *et al.*, 1973). At present it seems to be used to a lesser degree.

The second DE approach is the finite element (FE) method. Since the pioneering work of Coggon (1971) there have been published numerous works based on the FE method in geoelectromagnetic applications (e.g., Silvester and Haslam, 1972; Reddy and Rankin, 1973; Rodi, 1976; Kaikkonen, 1977, 1980; Reddy *et al.*, 1977; Pridmore *et al.*, 1981).

However, it seems that the most promising approaches to attack the problem of large computer requirements in solving complex 3D cases are hybrid methods, which try to combine good characteristics of DE and IE methods (Scheen, 1978; Lee *et al.*, 1981).

Thin sheet approximation (Price, 1949), which is an effective and useful way to consider distortions in EM field due to near-surface inhomogeneities, sedimentary layers and, oceans, has been used and developed progressively during about a decade (e.g., Schmucker, 1971; Weidelt, 1977; Vasseur and Weidelt, 1977; Weaver, 1979; Dawson and Weaver, 1979a; Ranganayaki and Madden, 1980; Fainberg and Zinger, 1981; Hermance, 1982b; Weaver, 1982).

In this review paper I shall initially summarize briefly those works published after the 6th Workshop of Electromagnetic Induction in the Earth and Moon held in August 1982 in Victoria, Canada. Numerical EM modeling was reviewed at Victoria in two extensive and excellent papers by Hohmann (1983) and Varentsov (1983). Because Hohmann (1983) presented theoretical formulations in a unified manner, both for the frequency and time domains, I shall not deal with formulations. In the second part, I shall define 'characteristic dimensions' – as I understand these two words in this connection – and consider some works in which I have found studies of them.

2. Numerical Modeling

The use of different numerical modeling programs (particularly 2D ones) is nowadays a routine tool in many kinds of EM induction work (e.g., Menvielle *et al.*,

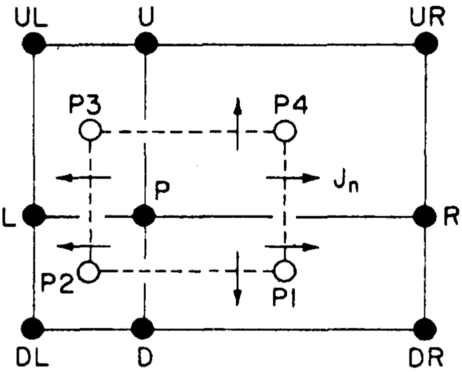

Fig. 1. The position of the temporary nodes (P1, P2, P3, P4) in each of the four regions surrounding the central node P. The surface of integration is shown as a dashed line, and the respective normal current densities J_n are shown as arrows (taken from Hermance, 1982a).

1982; Ádám *et al.*, 1982; Mbipom and Hutton, 1983; Ritz, 1983; Jödicke *et al.*, 1983; Červ *et al.*, 1984; Kaikkonen and Pajunpää, 1984; Schwarz, 1984). However, it is known, in spite of an almost everyday use of 2D forward modeling, that a real drawback in modeling of complex geoelectric structures is the great need of computer resources. This drawback of forward modeling is naturally one of the greatest obstacles for effective and routine use of 2D inversion techniques – without speaking about 3D inversion. Therefore it is quite natural that research in forward modeling is concentrating on improving and developing the modeling techniques in this respect. However, even today this seems to happen by using certain symmetry assumptions or other limitations for the model (Tripp, 1982; Tripp and Hohmann, 1984; Raiche and Tarlowski, 1984).

2.1. DE APPROACHES

Hermance (1982a, b, 1983, 1984) has presented a series of excellent papers. In the first of these Hermance (1982a) describes a finite difference form for simulating the behaviour of telluric fields near electrical inhomogeneities. Instead of using the conventional differential forms of Maxwell's equations, which result in five-point operators, he uses a local integration of the electric current density crossing a closed surface surrounding a mesh node (Figure 1). The resulting expressions for 2D models are accurate to second degree everywhere and have the form of nine-point FD operators, but have a higher precision than those derived from the usual differential forms with five-point operators. The comparison of an analytical solution with calculations using both the conventional five-point differential form and the developed nine-point form shows that in some cases there is an improvement of at least a factor of three when using the nine-point operator instead of the five-point operator (Figure 2 and Table I). Listed in Table I are values of the anomalous field relative to the source field

$$\Delta E_x = [E_x(x) - E_x(\text{source})]/E_x(\text{source}) \tag{1}$$

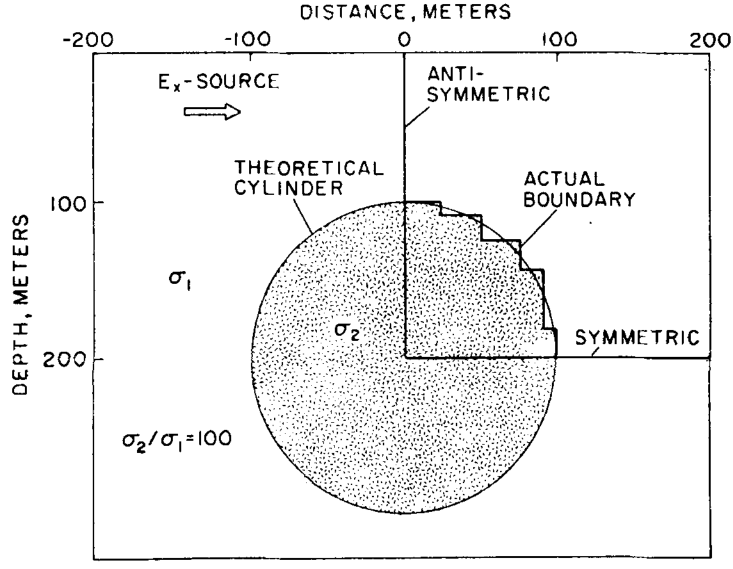

Fig. 2. The model of a horizontal cylinder for which analytical and numerical calculations are compared. The actual boundary of the numerical model consists of a series of rectilinear steps, as shown; the cross-sectional area, however, is the same as the cylinder shown. The radius of the cylinder was 100 m, and it was 100 times more conducting than its surroundings. Calculations were made along a profile 100 m above the top of the cylinder (200 m from its center). The actual model consisted of 18 × 18 nodes in only the upper right-hand quadrant and extended to 1000 m in both the horizontal and vertical dimensions (taken from Hermance, 1982a).

as a function of distance from a point directly above the center of the cylinder. In Table I is also listed the difference between each FD calculation and the analytical result as normalized residuals, e.g., the normalized residual for the five-point operation is given by

$$R_N^{(5)} = [\Delta E_x(\text{5-point}) - \Delta E_x(\text{anal.})]/E_x(\text{anal.}) \qquad (2)$$

and similarly for $R_N^{(9)}$. The table also summarizes the root-mean-square (rms) normalized residual of each FD result. This parameter is calculated by taking the square root of the mean of the normalized residuals squared. The reason for significant improvements in accuracy in regions of space where the fields are highly distorted, or where anomalous fields decrease rapidly with distance from a localized inhomogeneity, is that the integral form accounts for cross-derivative ($\partial^2 U/\partial x \partial z$) effects of the scalar potential U.

The assumption that the spatial wavelength of the source field, as well as the inductive attenuation distance associated with conducting media, are large compared to the scale size of the conducting inhomogeneity is used also in the papers by Hermance (1982b, 1983). The integral form FD technique developed by Hermance (1982a) for 2D models is used also by Hermance (1982b, 1983) in which the technique is extended to 3D models. The assumption that the skin depth δ ($\delta = \sqrt{2/\omega\mu\sigma}$) is much

TABLE I

Comparison of analytical solution to finite-difference calculations using differential and integral forms: Horizontal cylindrical anomaly. Radius = 100 m, depth to top of cyl. = 100 m, σ(cyl.) = 100σ(surroundings) (taken from Hermance, 1982a).

Distance (M)	Analytical solution	Differential form (5-point)		Integral form (9-point)	
	Anomalous field	Anom. field	Norm. resid.	Anom. field	Norm. resid.
0	−0.245	−0.257	4.9%	−0.248	1.2%
24	−0.235	−0.246	4.7	−0.238	1.3
40	−0.217	−0.228	5.1	−0.222	1.8
52	−0.200	−0.209	4.5	−0.204	2.0
76	−0.160	−0.166	3.8	−0.163	1.9
92	−0.132	−0.135	2.3	−0.134	1.5
100	−0.118	−0.120	1.7	−0.119	0.8
120	−0.0848	−0.0837	1.3	−0.0847	0.12
200	0.0	0.007	–	0.006	–
		rms norm. resid. = 3.8%		rms norm. resid. = 1.4%	

greater than the characteristic dimension L of the geologic structure ($\delta \gg L$) which Hermance (1982a, b, 1983) used means that he was dealing with the distortions of DC-type or galvanic fields and neglected self-induction and mutual induction effects.

The fourth paper mentioned above (Hermance, 1984) is important for EM induction studies from satellite altitudes. This topic has been developed rather recently (e.g., Hermance, 1982c). Hermance (1984) describes an approach to solving the case of EM induction by a time-varying 2D current source directed parallel to the strike of a 2D anomalous structure within the earth, i.e., the TE or E-parallel mode. The case which is considered is somewhat more generalized than most of the previous work, particularly when the satellite is above the source, and has not been studied up to the present time except for simple, 1D earth models. A finite source field is located at some position within the modeling region (Figure 3) and is simulated by discontinuities in the magnetic (or electric) field appropriate to the current flowing in the source. Boundary conditions expressed in Figure 3 have been established for the boundaries of the modeling region and then the unknown fields within that region have been solved using a developed FD algorithm. Figure 4 depicts the comparison of simulated satellite and ground-based observations of magnetic variations presented by Hermance (1984). An ionospheric current source is located at a height of 110 km. At satellite altitudes (400 km), the differences between the results for a uniform source (e.g., a remote magnetospheric source) and results for a finite source field below the satellite (ionospheric source) are profound. The total horizontal magnetic field produced by the distant source is approximately unity showing

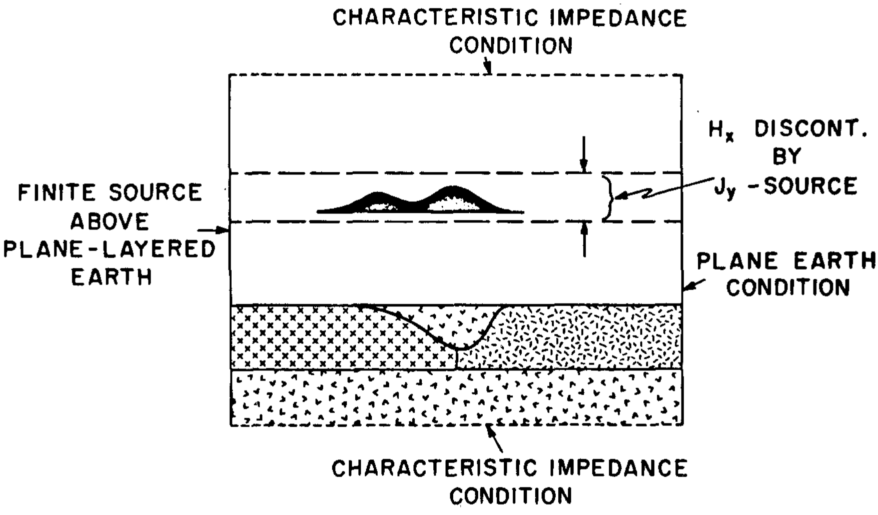

Fig. 3. Details of the model considered in the paper by Hermance (1984) (taken from Hermance, 1984).

insensitivity to lateral conductivity variations. The total horizontal field produced by an ionospheric source field is reduced by more than an order of magnitude. This reduction is due to the fact that the satellite is above the source thus the primary and secondary horizontal magnetic field components tend to cancel and the resultant field is fairly small. An anomalous vertical field produced by the ionospheric source is also small, but, however, of the same order of magnitude as the field produced by remote uniform sources in the magnetosphere.

Spichak (1982) presented a 3D algorithm based on the FD approximation of the vectorial equation governing the behaviour of the electric field. The system of linear equations is solved by means of an iterative successive blocked over-relaxation (SBOR) technique with dynamic correction of the relaxation factor. The primary source field can be a plane wave field or driven by the vertical magnetic dipole located at the surface of the earth.

The FE method is most likely better than the FD method in dealing with complex geoelectric structures, particularly in modeling different kind of sloping inhomogeneous bodies and interfaces and in treating the boundary conditions inside the modeling region. It seems, that the active and productive research of the FE method in EM modeling – at least on the basis of the small amount of the published FE papers – has reduced in recent years. I hope that this is only reflecting a situation "it is calm before a storm", since the FE method has potential to deal with real problems of complex nature.

Kaikkonen (1983) reviewed the 2D finite element modeling in magnetotellurics. A comparison between the FD results by Ádám (1981) and the FE results calculated by a higher-order (quadratic polynomials) isoparametric elements for the model in Figure 5a was presented by Kaikkonen (1983). That model is one of the 2D models (model 2D-4) proposed for comparison purposes by the so-called COMMEMI-

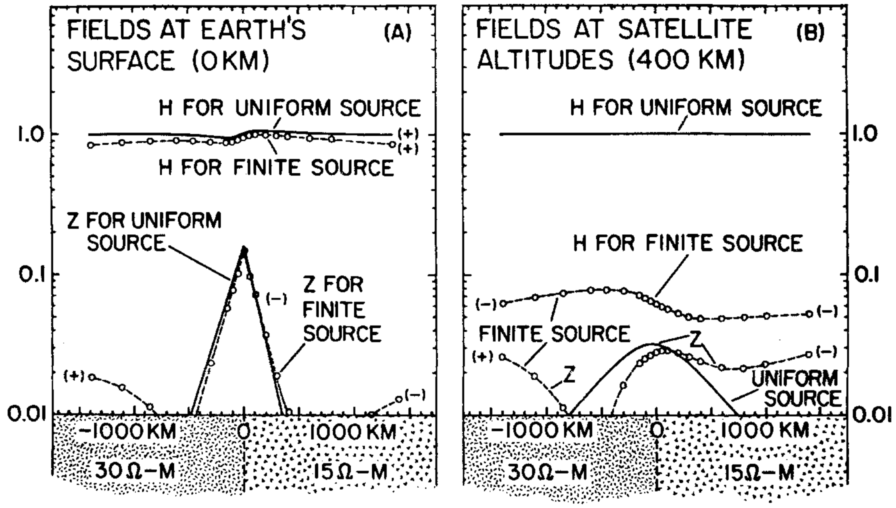

Fig. 4. Comparison of simulated satellite and ground-based observations of magnetic variations. The H field is horizontal and directed toward increasing x; the Z field is vertical and directed downward. The signs in brackets are associated with the various branches of the curves used to denote the amplitude of the respective field amplitudes. Panel A: H and Z fields observed on the earth's surface; Panel B: H and Z fields observed at satellite altitudes (400 km). All field amplitudes represent the sum of the source *and* the induced field components (taken from Hermance, 1984).

project of the WG I/3 of IAGA (Zhdanov, 1983). The H-polarization results by Kaikkonen (1983), and the additional ones calculated by Varentsov with his FD program (see ref. e.g., Zhdanov *et al.*, 1982) and by myself with the FD program written by Brewitt–Taylor (Brewitt–Taylor and Weaver, 1976; Weaver and Brewitt–Taylor, 1978) are here presented in Figures 5b–5e. The comparison shows that the results given by different programs differ particularly in the points $x = -6$ and $+5$ km, which are, of course, the most critical points in this comparison. The compatibility of the E-polarization results (not shown here) is very good.

Though the comparison of different numerical solutions is useful and important, the comparison of the numerical solution to the analytical one is of course very desirable, too. Figure 6 depicts the model used to compare Kaikkonen's FE results and analytical ones calculated with the program developed and written for the H-polarization by Weaver *et al.* (1985). Table II presents that comparison for the real and imaginary parts of the E_y component at the surface ($z = 0$) of the earth. We can see that the agreement between the FE calculation and analytic solution is excellent.

Although the time-domain EM (TDEM) methods offer many advantages over the frequency-domain methods (e.g., Kaufman, 1978; Stoyer and James, 1983), particularly in prospecting and upper crustal studies, the papers dealing with numerical TDEM modeling are still very uncommon (however, e.g., Kuo and Cho, 1980; Tripp, 1982). Since the excellent review paper by Hohmann (1983), in which he dealt thoroughly also with TDEM modeling, it seems that only one paper for TDEM modeling has been published, i.e., Goldman and Stoyer (1983). They used

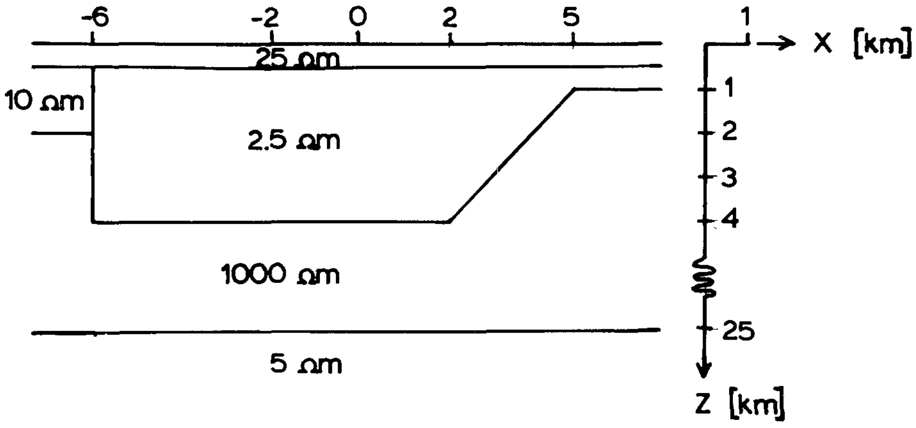

Fig. 5a.

Fig. 5(a)–(e). 2D model 2D–4 of the COMMEMI-project. MT soundings at the sites $x = -6, -2, 0, 2$, and 5 km are used for numerical comparison in Figures 5b–e. (b) *H*-polarization. FD method. Results by Ádám (1981). (c) *H*-polarization. FE method. Results by Kaikkonen (1983). (d) *H*-polarization. FD method. Results calculated by the program of Brewitt–Taylor and Weaver. (e) *H*-polarization. FD method. Results by Varentsov.

a FD formulation of the coaxial-loop or wire-loop transient EM prospecting systems to model the fields from a buried cylindrical conductor whose axis is coincident with that of the field system. Solutions were obtained directly in the time-domain. The formulation is implicit and 2D. The variable-directions method reduces each advance of one step in time from one 2D problem to a large number of 1D problems. This results in a reduction in computational effort. In order to avoid

TABLE II

Comparison of the analytical and FE solutions for the 2D *B*-polarization model presented in Figure 6. Analytical results were obtained by Weaver's program (Weaver *et al.*, 1984) and FE results by Kaikkonen's program.

	Analytical solution		FE solution	
Y[km]	E_y^{Re}	E_y^{Im}	E_y^{Re}	E_y^{Im}
−40	-0.3806×10^6	-0.3639×10^6	-0.3813×10^6	-0.3699×10^6
−30	-0.3801×10^6	-0.3628×10^6	-0.3809×10^6	-0.3688×10^6
− 7	-0.4082×10^6	-0.3685×10^6	-0.4091×10^6	-0.3739×10^6
− 3.7	-0.4346×10^6	-0.4084×10^6	-0.4358×10^6	-0.4190×10^6
− 2.14	-0.5106×10^5	-0.7897×10^5	-0.5140×10^5	-0.7531×10^5
− 0.9	-0.6369×10^5	-0.1147×10^6	-0.6487×10^5	-0.1180×10^6
0	-0.6474×10^5	-0.1199×10^6	-0.6563×10^5	-0.1231×10^6
0.9	-0.5876×10^5	-0.1132×10^6	-0.5992×10^5	-0.1164×10^6
2.14	-0.3931×10^5	-0.7237×10^5	-0.3952×10^5	-0.6794×10^5
4.1	-0.6009×10^6	-0.6488×10^6	-0.6020×10^6	-0.6592×10^6
8.5	-0.5574×10^6	-0.6066×10^6	-0.5581×10^6	-0.6121×10^6
18.0	-0.5228×10^6	-0.6056×10^6	-0.5235×10^6	-0.6119×10^6
50.0	-0.5121×10^6	-0.6211×10^6	-0.5127×10^6	-0.6274×10^6

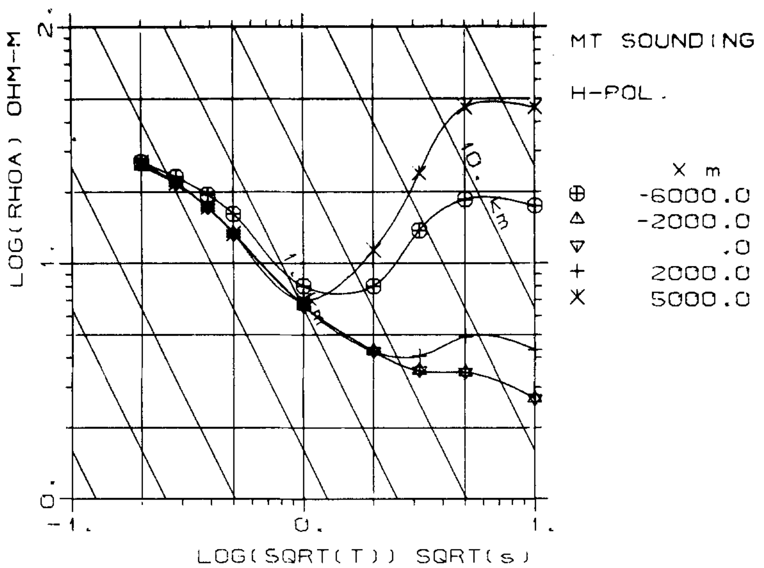

Fig. 5b.

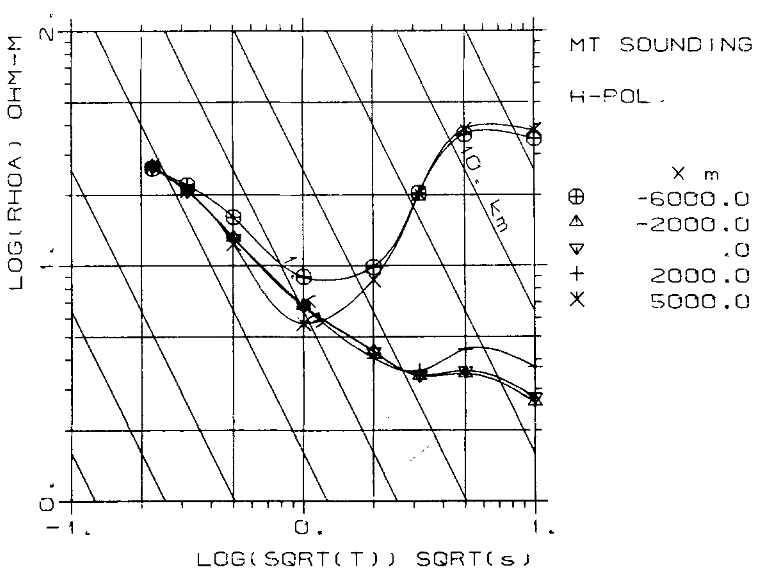

Fig. 5c.

including the air in their FD mesh they used an integral equation approach to formulate the surface boundary conditions. Hence two sets of 1D finite difference solutions and one Fredholm integral equation solution are required for each step forward in time. They compared their calculations to analytical solutions with excellent agreement in the case of four-layer earth.

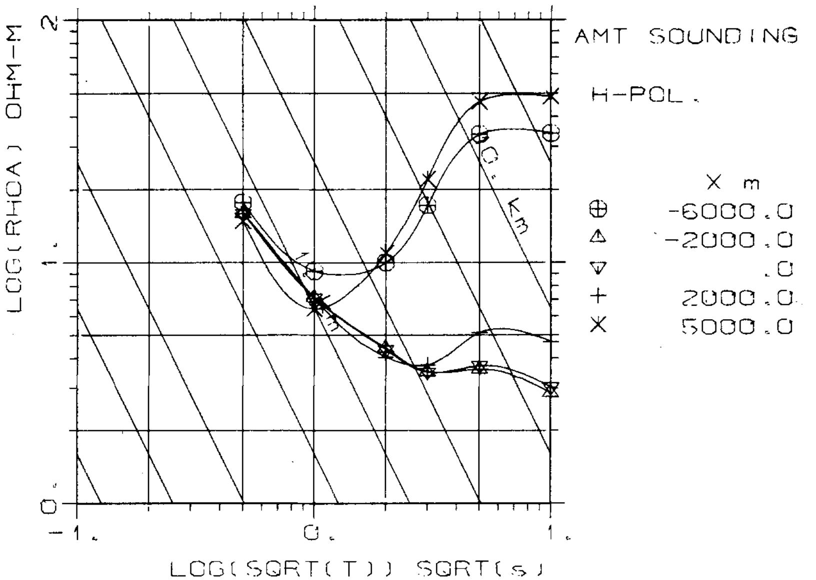

Fig. 5d.

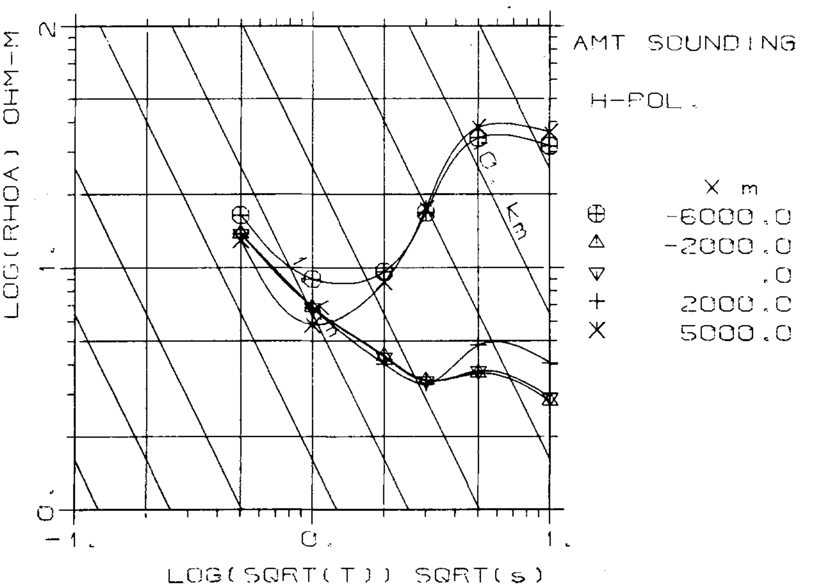

Fig. 5e.

2.2. IE METHODS

In IE techniques the target – the inhomogeneous body – is divided into cells. Because the size of the cell has to be less than a skin depth in that body and on the other hand less than the depth to the top of the cell, matrix computation time and storage can be excessive (Hohmann, 1983). For example, the division of the body into

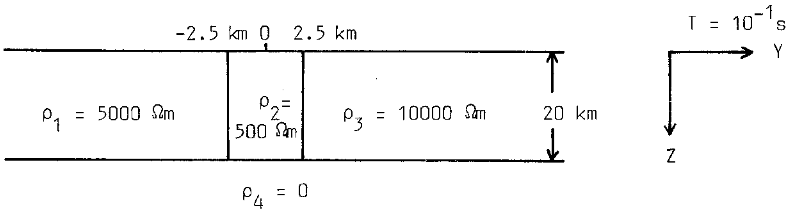

Fig. 6. The 2D model used for the comparison between the FE and analytical solutions presented in Table II. The B-polarization. The period is $T = 10^{-1}$ s.

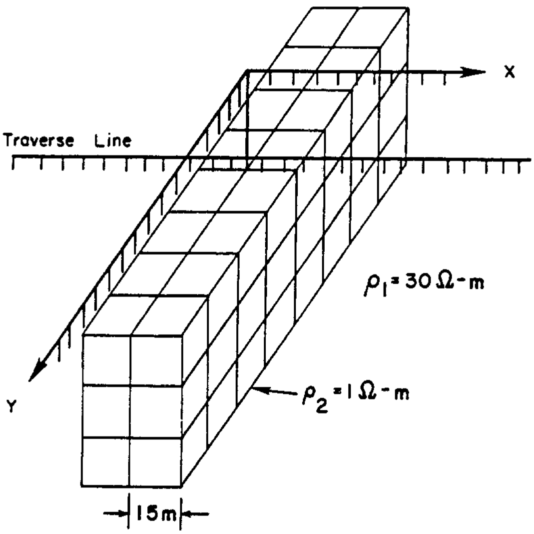

Fig. 7. Test model buried 30 m and discretized by 15 m cubes (taken from Tripp, 1982).

N cells generates a full matrix of dimension $3N \times 3N$ and the matrix factorization time increases as N^3 while the matrix formation increases as N^2 (Tripp and Hohmann, 1984). Tripp (1982) and Tripp and Hohmann (1984) studied the conditions under which the general full-matrix equation

$$\bar{\bar{Z}}\bar{J} = \bar{E}^i \tag{3}$$

assumes a simpler form. Equation (3) gives the vector of incident electric field values $\bar{E}^i$ at the centres of the cells which comprise the anomalous body as the linear transformation of the vector of total electric current values $\bar{J}$ at the centres of the cells. The transformation matrix $\bar{\bar{Z}}$ is called the impedance matrix. If the horizontal cross sections of a body with vertical sides all possess a certain symmetry, the $\bar{\bar{Z}}$ matrix contains information about the effect of the symmetry on the scattering currents. This information can be deduced easily using group theory independent of any numerical computation or particular incident field geometry, and the original

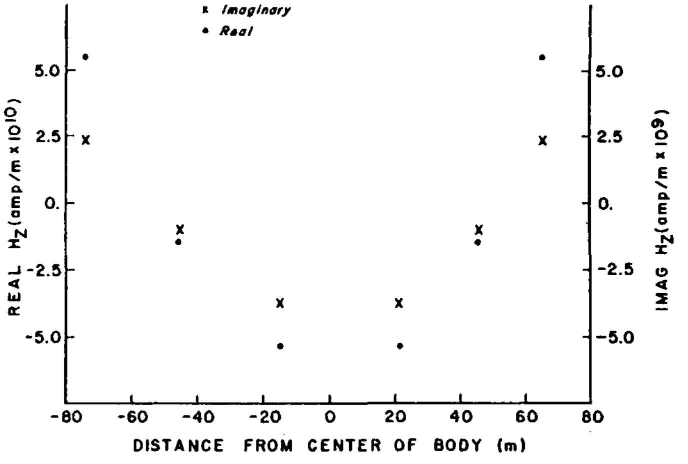

Fig. 8. Real and imaginary components of the secondary H_z response of the body and traverse of Figure 7. The real components are denoted by dots while imaginary parts are denoted by crosses. Both components are plotted at the x value midway between the transmitter and receiver. The source is a vertical magnetic dipole at the frequency of 100 Hz (taken from Tripp, 1982).

matrix, containing redundant information, can be replaced by a block-diagonal matrix (see details Tripp, 1982; Tripp and Hohmann, 1984).

Tripp (1982) and Tripp and Hohmann (1984) gave the numerical example for the model in Figure 7 with results in Figure 8. This example shows how the computer storage requirements and solution time for the block-diagonalized matrix equation are significantly smaller than those for the original matrix equation without using symmetry (Table III). The dimensions of the scatterer in Figure 7 are

TABLE III

Comparison between algorithms using symmetry and not using symmetry (taken from Tripp, 1982).

	Using symmetry	Not using symmetry
Total Matrix Storage (Words)	10368	41472
Matrix Formation Time (Cpu secs)	29.8	95.6
Matrix Factorization Time (Cpu secs)	3.5	41.3
Surface Field Evaluation Time (Cpu secs)	16.8	17.2
Total Computation Time (Cpu secs)	68.1	156.3
Total Cost	$1.32	$5.82

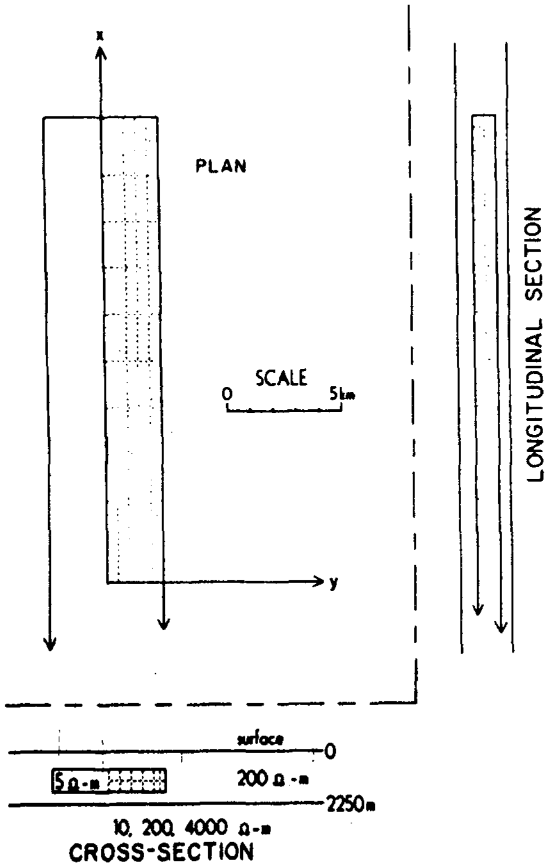

Fig. 9. Elongate 3-D body. Dashed lines show rectangular cell discretization with only half of the body shown in plan and longitudinal section. The smaller cells near the center give greater accuracy to the scattered fields along the y axis over the edge of the body. The strike length is 40 km, depth is 750 m, depth extent is 1750 m, and width is 5 km (taken from Wannamaker *et al.*, 1984a).

$30 \times 120 \times 45$ m and its center axis lies along the z-axis. The source was a vertical magnetic dipole at the frequency of 100 Hz. The response was calculated for six transmitter sites on the traverse line $y = 30$ m, while the receiver for each transmitter site was located 120 m in $+x$ direction from the transmitter. Figure 8 depicts the real and imaginary parts of the field component $H_z(x)$, when the group theory was used. The component values are plotted at the x value midway between the transmitter-receiver range. The comparison in Table III is made for a single receiver site (a UNIVAC 1100/61 computer was used in calculations).

Wannamaker *et al.* (1984a) published the paper dealing with EM modeling of 3D bodies in layered earths. They used an IE technique, and showed amongst other things that the use of rectangular cells instead of the usual cubes is useful for approximating elongated inhomogeneities, since variations in the total electric field are more abrupt across shorter dimensions of the body than across longer ones. Furthermore, they found that tabulation and interpolation of the six electric and five

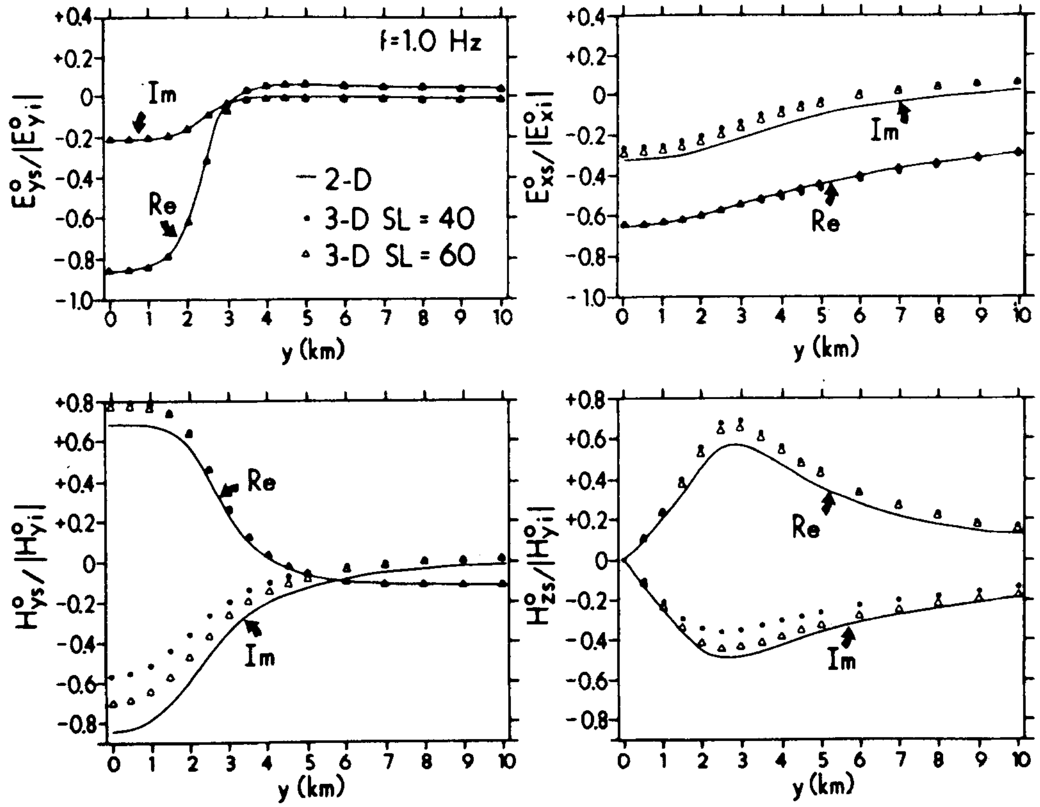

Fig. 10. Profiles of normalized real (Re) and imaginary (Im) secondary electric and magnetic field components at 1.0 Hz along the y axis of the 3-D body of Figure 9, a similar 3-D body of SL = 60 km, and across a 2-D body of identical cross section for a basement resistivity of 4000 Ωm. The response of the 60 km long 3-D body, plotted using open triangles, shows improved convergence over the response of the 40 km long body with the 2-D transverse electric results (taken from Wannamaker *et al.*, 1984a).

magnetic Hankel transforms provide a much more efficient means of computing the Green's function than does a direct transform evaluation using linear filters or any other method. Still they concluded that the length which a 3D body must have before departures between 2D transverse electric (i.e., TE or E-parallel mode) and corresponding 3D signatures are significant depends strongly on the layering, but the 2D transverse magnetic (i.e., TM or H-parallel mode) and corresponding 3D results agree closely regardless of the layered host.

The model they used is depicted in Figure 9. The plate-like inhomogeneity (1000 m thick, at a depth of 750 m, width 5 km, strike length 40 km) is located in the upper layer of a two-layer earth. Plane-wave excitation at the frequency of 1 Hz was used. An example of their comparisons between surface fields from 3D body and the corresponding 2D structure by changing the basement resistivity (being 10, 200, and 4000 Ωm) and also the strike length (SL) (SL = 40 and 60 km) is shown in Figure 10. Wannamaker *et al.* (1984a) used the FE routine (Rijo, 1977; Stodt, 1978) in calculating the 2D fields. The secondary electric field E^0_{ys} in the y direction corresponds in the 2D case to the TM mode of excitation and has been normalized in the plots by the incident electric field magnitude at the earth's surface $|E^0_{yi}|$. The TE mode components E^0_{xs}, H^0_{ys} and H^0_{zs} have been normalized respectively by $|E^0_{xi}|$, $|H^0_{yi}|$ and $|H^0_{yi}|$.

Wannamaker *et al.* (1984b) studied magnetotelluric responses of 3D bodies in layered earths using the computer program of Wannamaker *et al.* (1984a). They developed magnetotelluric theory for 3D bodies buried in 1D media establishing the fundamental controls on observed responses, and investigated the utility of 1D and 2D algorithms for interpreting 3D geology. They concluded that relative to the TE response of a 2D body of identical cross-section, the apparent resistivity identified as TE by conventional means over and around a confined 3D conductive body suffers a widespread depression that is increasingly pronounced toward lower frequencies. This depression of the 3D response results from current-gathering. Interpretation of such a 3D response using 1D or 2D TE modeling approaches can imply erroneously low resistivities at depth below the true inhomogeneity. Thus, they made a conclusion that many published models of deep resistivity derived from MT have experienced a bias toward shallow, low resistivities. Accordingly, it is quite obvious that in the near future – or better to say that when we shall have in our every day usage 3D programs – we must reinterpret many MT anomalies.

2.3. Hybrid Methods

A new hybrid method – the *s*ummary *r*epresentation *h*ybrid *m*ethod (SRHM) – combining the method of summary representation and FD technique was described by Raiche and Tarlowski (1984) and Tarlowski *et al.* (1984) and used to solve the Helmholtz equation on a 2D rectangular domain.

For the problem of a small central subdomain with locally varying γ ($\gamma^2 = i\omega\mu\sigma(x, y)$ surrounded by larger subdomains in each of which γ is a constant (Figure 11) one would like to use a local FD or FE method combined with a more efficient, perhaps analytic, method over the rest of the whole domain.

For a limited class of discretization procedures, the method of summary representation can be used to find analytical solutions to FD analogs of many of the differential equations of mathematical physics.

In general, the method consists of finding an analytical solution to the 1D FD eigenvalue problem. For self-adjoint FD boundary value problems expressed over N points, a basis of N orthogonal eigenvectors, corresponding to N distinct real eigenvalues, can be found. These functions, expressed as a matrix of N eigenfunctions at N points, form the basis of the so-called P transform.

The 2D problem is solved by using a five-point difference scheme to discretize the equation over a mesh with N interior points in the x-direction and M interior points in the y-direction. This gives a system of MN equations in which the x and y variations are coupled. The boundary values at $x = x_0$, $x = x_{N+1}$, $y = y_0$ and $y = y_{M+1}$ are assumed to be known.

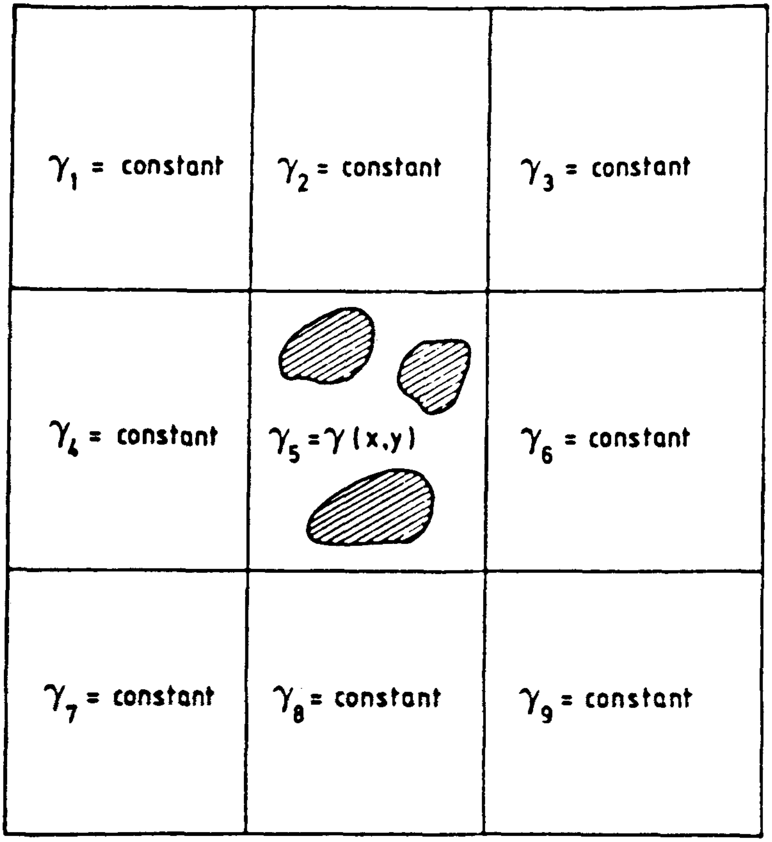

Fig. 11. Division of large domain into appropriate subdomains (taken from Raiche and Tarlowski, 1984).

Applying the P transform to that system of equation decouples the x and y variations into M systems of N equations in one variable. But since each of these resulting 1D equations can be solved analytically, the solution at any given point in the whole region can be expressed in analytic form in terms of the 1D eigenfunctions and the boundary values.

Furthermore Raiche and Tarlowski (1984) described the course of the summary representation for the 2D Helmholtz equation. They stated that the method of summary representation works only for a limited class of discretization procedures because of the difficulty of finding analytic eigenfunctions for the 1D problem. Thus they had to use constant mesh spacing in x and y-directions and constant $\gamma(x, y)$ on the rectangular subdomain. Due to uniform discretization in the y-direction and constant $\gamma(y)$ their 1D FD equation defined over M points with known boundary conditions of y_0 and y_{M+1} (top and bottom of the mesh) had constant coefficients and was therefore easy to solve analytically. Similarly, their restriction of uniform x discretization and constant $\gamma(x)$ allowed them to find the P transform analytically.

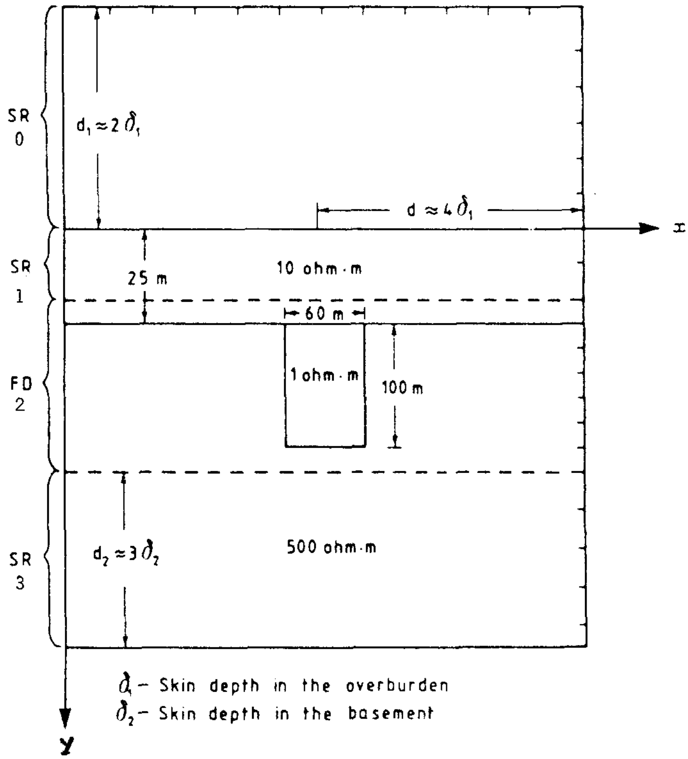

Fig. 12. Two-dimensional model for SRHM calculation. δ_1 = skin depth in overburden; δ_2 = skin depth in basement; FD = finite difference method; SR = summary representation; (taken from Raiche and Tarlowski, 1984).

Raiche and Tarlowski (1984) developed the formal solution to the block hybrid scheme, but as they stated that version of SRHM exists only in theoretical form at that moment. Thus they presented a geophysical example by applying the layered version of SRHM to calculate a model depicted in Figure 12. In the absence of the anomalous block in layer 2, the model has an analytic solution which was used to give the boundary values on all four sides of the total domain. The summary representation layers were given vertical discretizations of 0.1 δ_j (where $\delta_j = \sqrt{2/\omega\mu\sigma_j(x, y)}$, i.e., the skin depth) with the exception of layer 0 which was discretized at 0.1 δ_1. The FD layer was discretized at 0.2 δ_T, where δ_T was the skin depth in the target. The horizontal discretization was constant. Due to the type of boundary conditions, the accuracy of the model was much less sensitive to horizontal discretization than it was to vertical one.

Table IV shows the results of the comparison between the speed of SRHM and that of the FD method used for the whole domain. Raiche and Tarlowski (1984) ran four different models for $N = 21$, 41, 61, and 81, where N is the number of nodes in the horizontal direction (a VAX 11/780 computer was used).

Although the ratio of nodes in the FD layer to the total number of nodes in all four layers of the domain remained constant, the solution time should increase as the cube

TABLE IV

Comparison of computation times for hybrid and finite difference methods (taken from Raiche and Tarlowski, 1984).

Total number of internal nodes	Number of internal nodes in the layer with an inhomogeneity	Time in seconds for the hybrid method	Time in seconds for the finite difference method
1323	231	44.51	73.51
2583	451	101.40	294.70
3843	671	270.50	853.8
5103	891	529.04	1934.00

of the number of FD nodes and as the square of the number of summary representation nodes. Hence, as N increases, SRHM will have an increasing speed advantage over the FD method used alone. Table IV shows that SRHM was about 3 or 4 times faster than a conventional FD method. Raiche and Tarlowski (1984) also tested the accuracy of SRHM for layered models having analytic solutions. SRHM was more accurate than the FD solution. They concluded that SRHM offers more geometric flexibility than hybrid methods combining integral equation solution with finite elements.

2.4. Thin Sheet Approximations

Dawson *et al.* (1982) presented a new analytical solution for an H-polarization induction problem, in which a local region of the earth is represented by a generalized thin sheet at the surface of and in electrical contact with a uniformly conducting half-space. Their model (see Figure 13) included, for the first time analytically solved, the

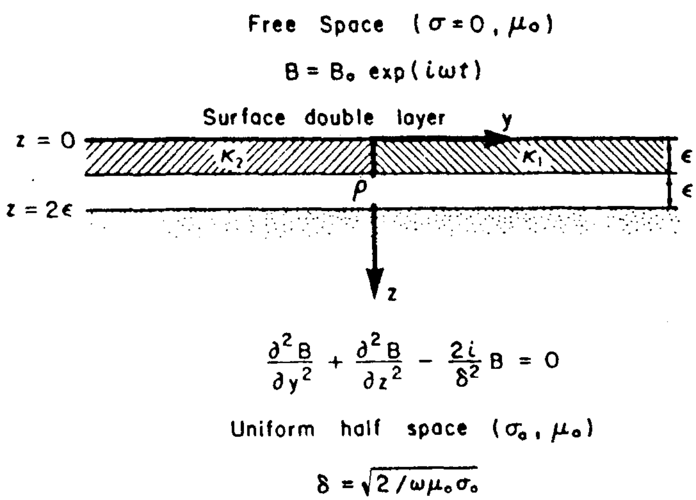

Fig. 13. The mathematical model: the generalized thin sheet in the plane $z = 0$ is obtained by letting $\epsilon \to 0$ (taken from Dawson *et al.*, 1982).

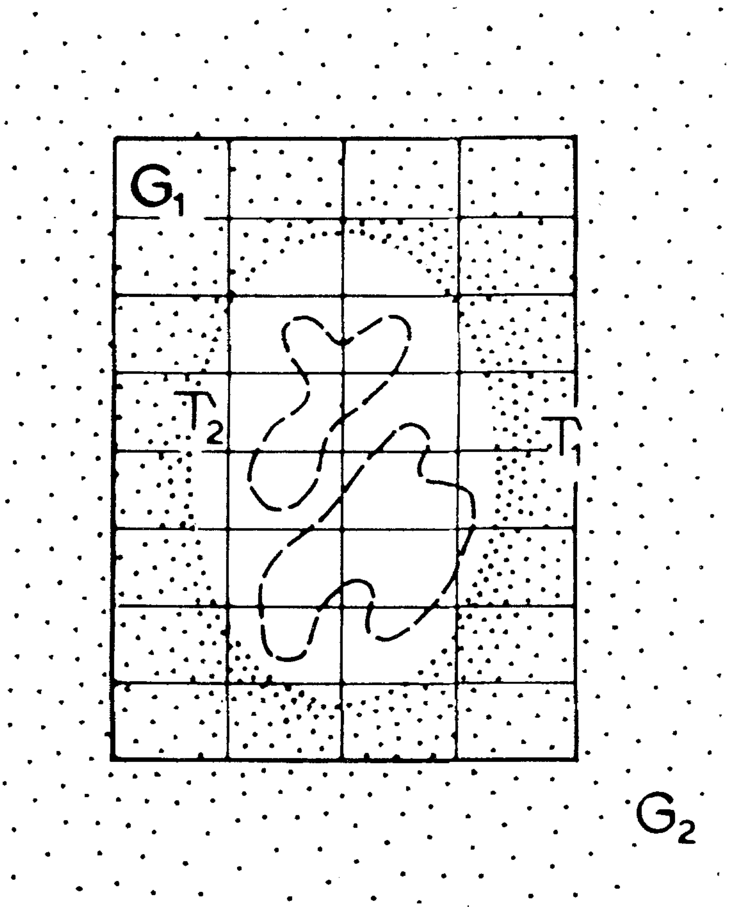

Fig. 14. The domains used in the proposed method: G_1 is the rectangular grid for the numerical solution, with Γ_1 being the boundary of G_1; the dotted area G_2 is the domain for the analytical solution with the ellipse Γ_2 as the inner boundary. The inhomogeneities in the conductance are shown by dashed lines (taken from Yegorov *et al.*, 1983a).

effect of both the conductive and resistive components of the earth's crust combined together in a single generalized thin sheet of the type first suggested by Ranganayaki and Madden (1980).

Dawson (1983) obtained also an analytical solution, but for the *E*-polarization problem of EM induction in two thin half-sheets underlain by a uniform conducting half-space. Dawson and Weaver (1979b) have solved the same model for the *H*-polarization mode. Thus Dawson's solution completes the study of 2D induction for that model. It also extends the analytic *E*-polarization solution of Weidelt (1971) by the inclusion of an underlying conductor and that of Raval *et al.* (1981) by the inclusion of arbitrary conductance values for the two surface sheets. This solution may be used as an idealized model of the coast effect and allows detailed study of the field behaviour near the discontinuity.

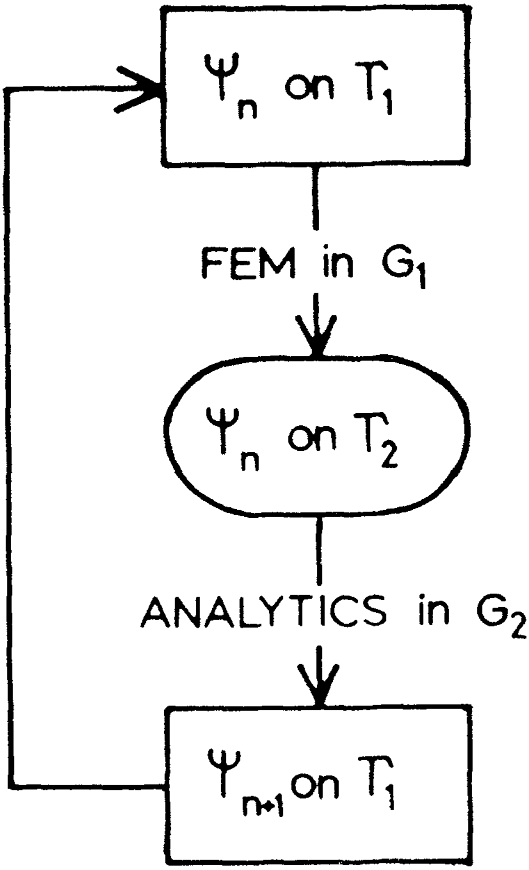

Fig. 15. The main scheme of the iterative process in the Schwarz method (taken from Yegorov *et al.*, 1983a).

Yegorov *et al.* (1983a) developed a thin sheet approximation using the hybrid technique by combining, in an iterative sense, the FE solution in the inhomogeneous part of the thin sheet and the analytical solution outside it. The low-frequency telluric field was obtained by solving the Price's equation using that hybrid technique. A neglect of self-induction and inductive coupling between currents in the sheet, as well as of poloidal current flow was made.

Figure 14 shows a simple illustration of the domains used in the approach of Yegorov *et al.* (1983a). The essence of the iteration process of the hybrid technique is presented in Figure 15. If it is assumed that ψ_n are the values of the current function on the boundary Γ_1 of the grid G_1 (see Figure 14) it is possible to obtain all the values of ψ inside Γ_1, i.e., in the grid G_1 by a numerical technique, i.e., by the FE method. After this approach the current function values are known on the ellipse Γ_2. Using these values the outer Dirichlet problem is solved analytically in the area G_2 outside of the ellipse Γ_2, where the conductance is constant. Now, new values can be obtained for the current function on the rectangular boundary Γ_1. Yegorov *et al.* (1983a)

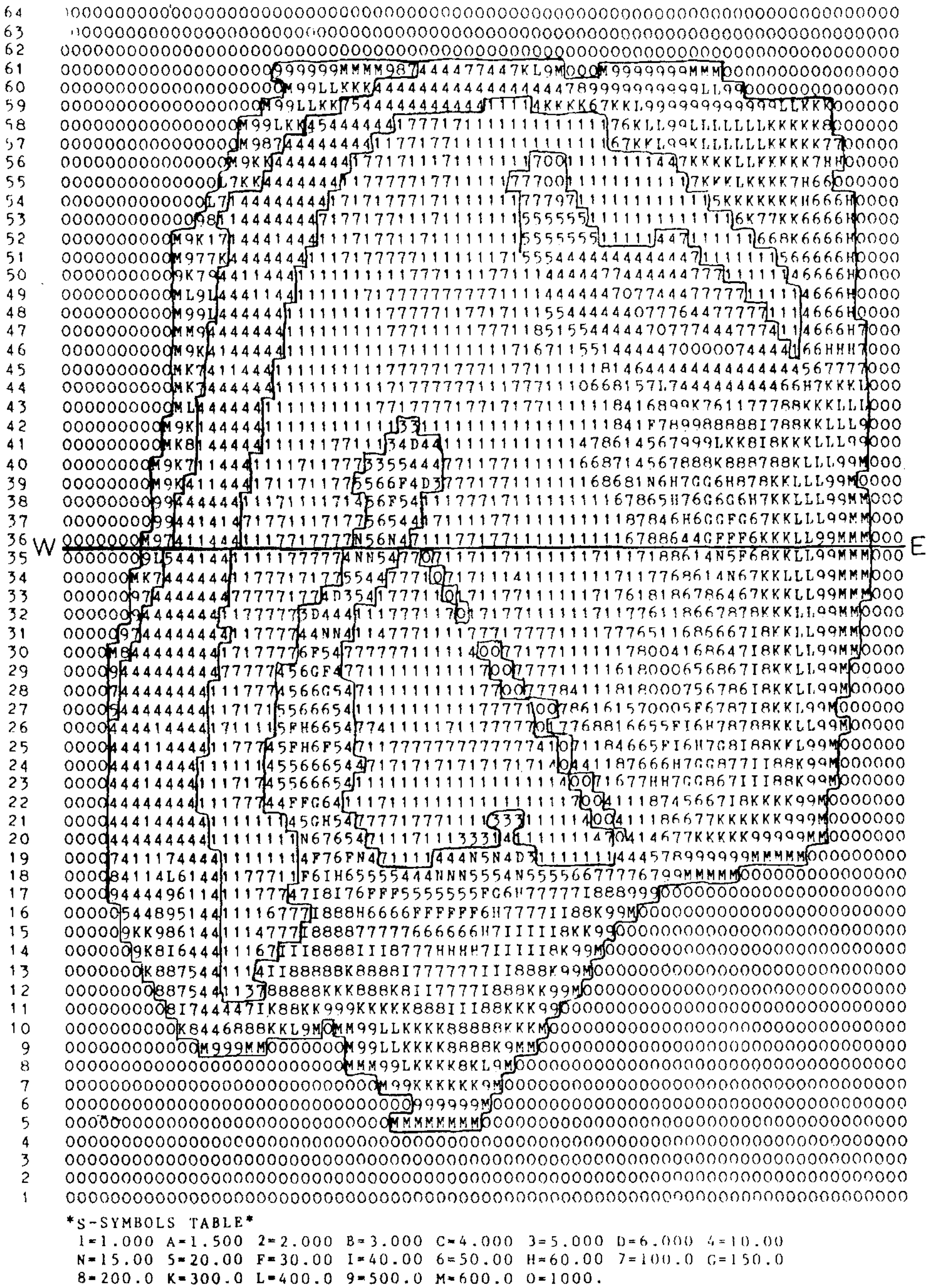

Fig. 16a. The conductance model for the Baltic Shield and the surrounding areas. Results for the W–E profile are presented in Figure 16b (taken from Yegorov *et al.*, 1983a).

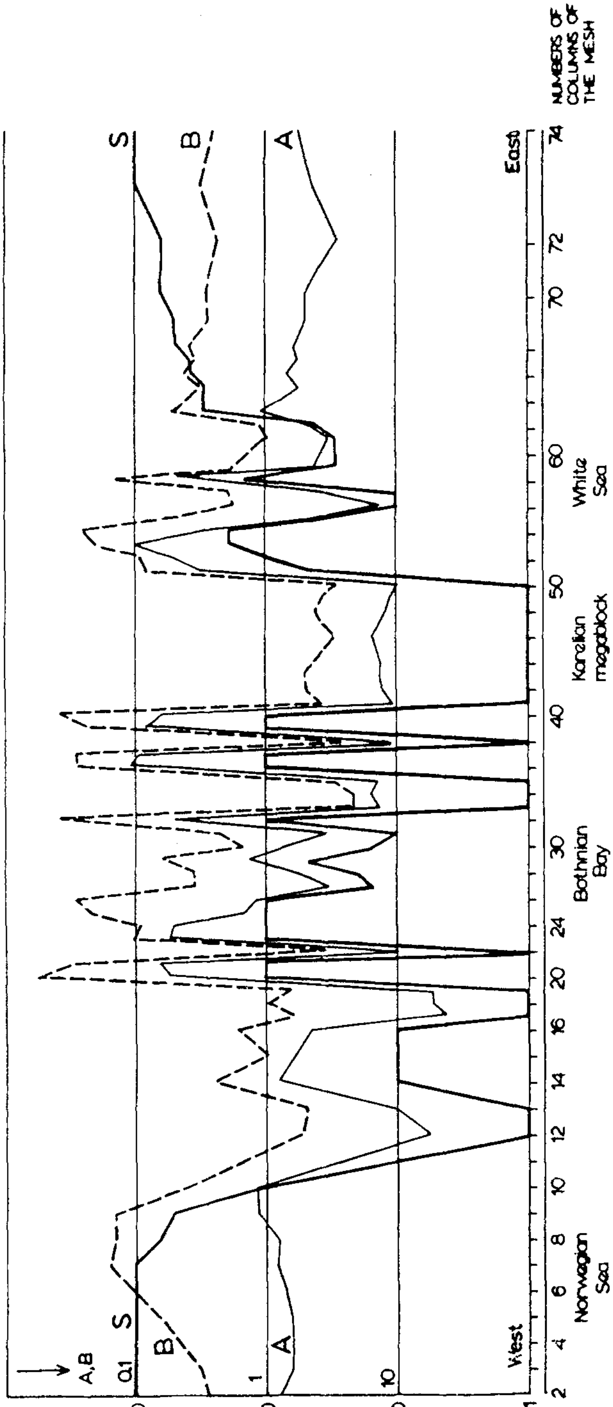

Fig. 16b. The conductance values (thick solid line), the major semi-axis *A* (solid line) and the minor semi-axis *B* (---) of the telluric ellipses along the W–E profile (see Figure 16a) (taken from Yegorov *et al.*, 1983a).

presented one example of their calculation for the Baltic Shield (Figure 16). Figure 16a depicts the conductance model for the Baltic Shield and Figure 16b shows the conductance, major semi-axis A and minor semi-axis B of the telluric ellipse along the W–E profile in Figure 16a. This profile shows a very distorted telluric field. The computer listings and a test run of their thin sheet program have been published by Yegorov *et al.* (1983b).

Using the thin sheet computer program developed by Yegorov *et al.* (1983b), Kaikkonen *et al.* (1984) analysed and compared the experimental MT data and theoretical data for the Kamchatka Peninsula proposing that the DC-type distortions of the telluric field play the most important role in the structure of the MT field in that area. Kaikkonen (1984) and Kaikkonen *et al.* (1985) have used the thin sheet approximation to study the distortions in the low-frequency telluric field due to variations in the near-surface conductance values at the Baltic Shield and the Rheingraben area, respectively. Mareschal and Vasseur (1984) reported on the use of the thin sheet approximation for modeling bimodal EM induction in non-uniform thin sheets embedded in a layered half space. They applied their algorithm to Scotland.

3. Studies of Characteristic Dimensions

First it is necessary to put a question "what are characteristic dimensions (CD) associated with EM induction in the earth?" Then we must consider three topics which are contained in the consideration of the EM induction problem:

(1) Source fields;
(2) Numerical modeling;
(3) Physical phenomena in the earth and interpretation.

In the following I will briefly consider and summarize studies of characteristic dimensions in each of these topics, though often, it is difficult to classify works exclusively into a certain topic. However, the third topic is the most important in considering 'characteristic dimensions' and it is usually connected with them. But before that I should term the depth of penetration (skin depth) of EM energy, in general, the most important and fundamental characteristic dimension. First, all information that is possible to obtain from anomalous structures through EM methods is based on the attenuation (skin effect) of EM waves in conducting media. Secondly the skin depth concept, has regularly been associated with almost all studies of characteristic dimensions and their definitions.

3.1. CD AND SOURCE FIELDS

In basic MT theory the primary source field is assumed to be a plane EM wave impinging on the flat surface of a horizontally layered earth. This is the so-called 1D Tikhonov–Cagniard model. The assumption of the plane wave nature of the MT source field has been critized by Wait (1954) and Price (1962). They showed that certain corrections are required at long periods for sources of finite size. Dmitriev and Berdichevsky (1979) finally pointed out that the principal condition in MT is the

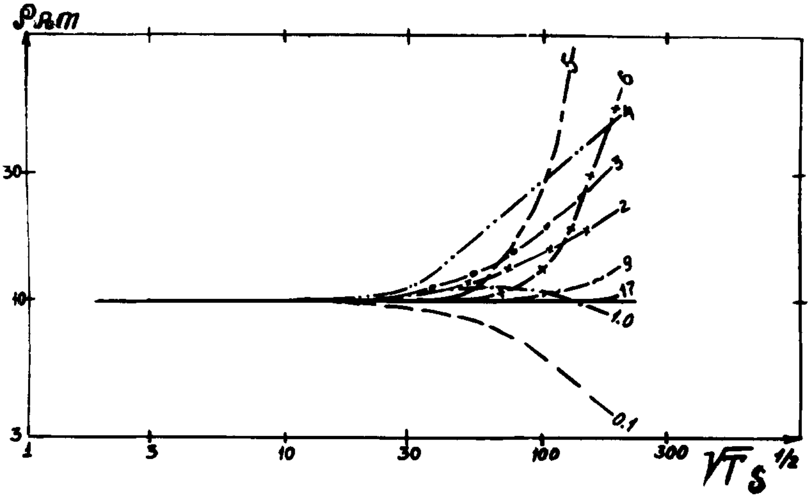

Fig. 17. The apparent resistivity curves, ϱ_a^1, calculated for an ionospheric arc. The earth is a homogeneous half-space with the resistivity $\varrho = 10\ \Omega$m. The curve parameter is r/h_0 (taken from Osipova, 1983).

linearity of the horizontal field variations and not the slowness of variation. They stated "if on the surface of a homogeneous earth H_x and H_y vary linearly over distances of the order of three times the field penetration depth δ, the ratios E_x/H_y and E_y/H_x determine the Tikhonov–Cagniard impedance irrespective of the relations between the H and the E modes".

Osipova (1983) studied the influence of ionospheric source field structure on deep MT results. She considered, among other things, the possibility of using the Tikhonov–Cagniard MT model under an ionospheric current arc with leakage current, when the arc size is 90°. The apparent resistivity curves, ϱ_a^1, calculated along the profile passing through the centre of the arc are presented in Figure 17, where the curve parameter is r/h_0, the ratio of the distance from the electrojet and the source height over the earth's surface. We can see that the ϱ_a^1 curves coincide practically with the curves for the plane wave, ϱ_a^{pw}, (half space $\varrho = 10\ \Omega$m) at all periods $T \leq 1$ hour, except in the region of the sign change of horizontal electric and magnetic components. At the longer periods the ϱ_a^1 and ϱ_a^{pw} are the closer to each others the larger is the parameter r/h_0.

Mareschal (1981) used scale lengths of 3D source field to study the validity of geomagnetic deep soundings at sub-auroral latitudes.

Hermance (1978) studied effects of moving ionospheric current systems on magnetotelluric measurements. Moving sources have positive effects on them. He found this result fairly surprising especially, when the depth of penetration, which was on the order of 500 km, was equivalent to the width of the source. As a moving source tends to average the induction phenomena over a larger volume than a stationary source, its effective width can be much broader than the width of the actual source itself. This results in the ability of the fields to penetrate to a much larger depth

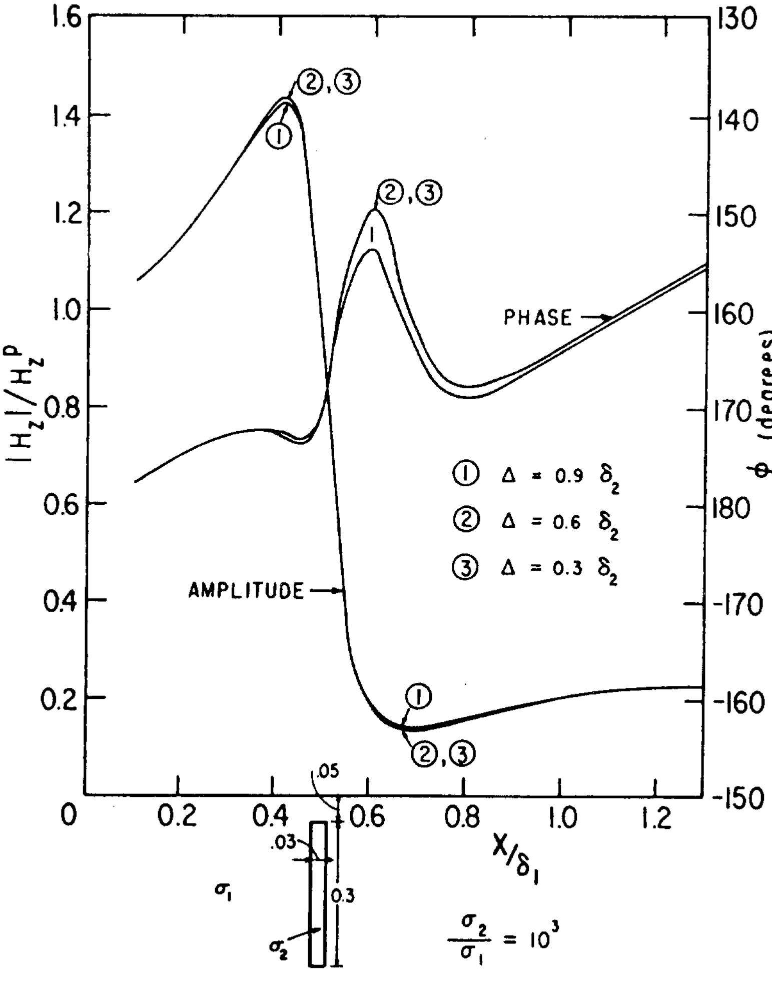

Fig. 18. Effect of cell size on accuracy of solution (taken from Hohmann, 1971).

before becoming constrained by the source geometry. Thus for a given source width the MT relation is valid to longer periods when the source is moving.

3.2. CD OF NUMERICAL MODELING

CD of numerical modeling means connections between the skin depth and dimensions of the mesh and elements or node spacings in the mesh. The accuracy of the numerical approximations for each problem is dependent on, these relations. Next I present some studies in this respect.

Hohmann (1971) presented the effect of cell size (S) on the accuracy of IE method. He considered the line source problem for 2D model and checked the accuracy by making computations for the same body with different values of S. Figure 18 depicts normalized H_z amplitude and phase (ϕ_z) for S values of 0.9 δ_2, 0.6 δ_2, and 0.3 δ_2,

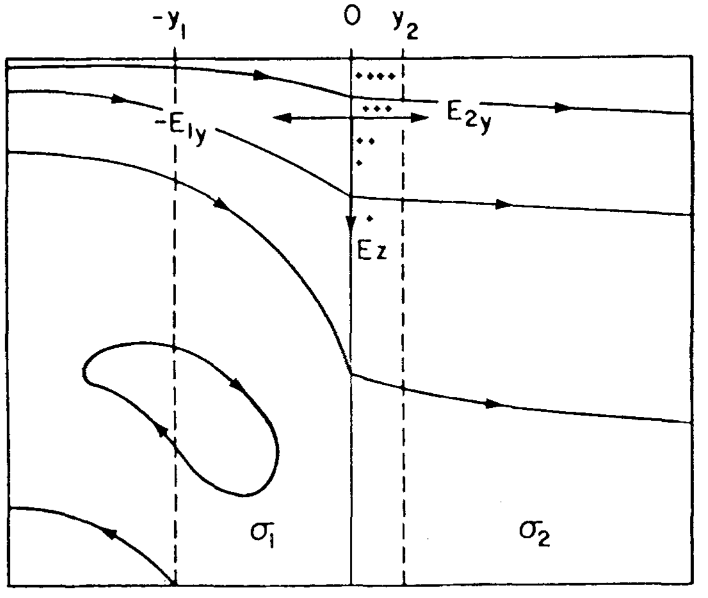

Fig. 19. Current lines and surface charge distributions near a vertical discontinuity in conductivity (taken from Jones, 1983).

where δ_2 is the skin depth in the conductor. Hohman (1971) concluded that, in general, a cell size of one-half to one conductor skin depth is sufficient.

In DE approximations the dimensions of the mesh used are also important. The skin depth of the host usually determines them. For 2D cases e.g., Coggon (1971) and Kaikkonen (1980) have presented the 'rules' some 3–4 skin depths of the host (δ_h) for the vertical sides from the nearest lateral conductivity contrast. The bottom of the mesh should be some 3–5 δ_h and the top of the mesh (thickness of the air layer in the E-polarization) at least 6–7 δ_h. None of these measures are quite absolute, but they depend somewhat on the conductivity contrasts and geometry of the model, as well as the boundary conditions used (e.g., Weaver and Brewitt–Taylor, 1978). The upper bound for the length of the sides of the elements used in the mesh is some 0.5–0.8 δ (e.g., Kaikkonen, 1980).

The basic requirement for the validity of the thin sheet approximation to be assured is that the tangential electric field is so little attenuated through the surface layer that its behaviour is reasonably consistent with the mathematical condition of continuity across a thin sheet (Weaver, 1979). Schmucker (1970) has shown that this requirement is met if the skin depth of the surface material is large compared to the thickness of the thin sheet (surface layer) and the depth of penetration of the field into the underlying medium is also large compared to the thickness of the thin sheet. Weaver (1982) considered also this question with the same results.

3.3. CD OF PHYSICAL PHENOMENA IN THE EARTH AND IN THE INTERPRETATION

Jones (1983) presented an excellent review paper at Victoria in 1982 on the problem

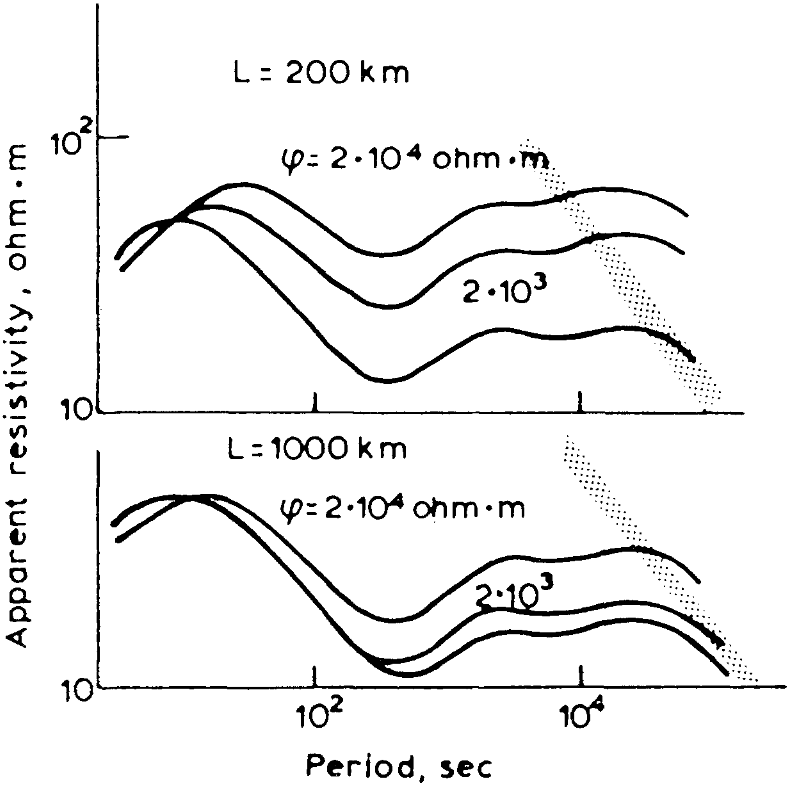

Fig. 20. Distortion of the apparent resistivity curves by near-surface inhomogeneities. Thick solid line is undistorted curve. Shaded band is the normal apparent resistivity (taken from Vanyan, 1981).

of current channelling in which he considered also quite thoroughly an 'adjustment distance', which has been probably the most used and well-known name of characteristic dimensions. Jones (1983) considered and presented the adjustment distance or 'equilibrium distance' based on Price's (1973) presentation (Figure 19). For points out with the two bounds $-y_1$ and y_2 in Figure 19 the current flow (in the H-polarization) has adjusted such that it is in equilibrium with that expected in a homogeneous half space of σ_1 (region 1) or σ_2 (region 2). Thus the distances y_1 and y_2 may be thought of as the adjustment distances or equilibrium distances, and a 1D interpretation of the response function E_y/H_x observed at $y < -y_1$ or $y > y_2$ will yield the correct conductivity. However, an interpretation of E_y/H_x observed within the bounds $-y_1 < y < y_2$ will not yield either σ_1 or σ_2 due to the perturbation of the current flow at the boundary (Jones, 1983). Similarly Jones (1983) extended that 2D illustration of a current perturbation effect to 3D model.

Now, the problems are determining of the range (y_1, y_2) and investigating when 1D or 2D interpretations are valid in 3D cases, i.e., research of characteristic dimensions.

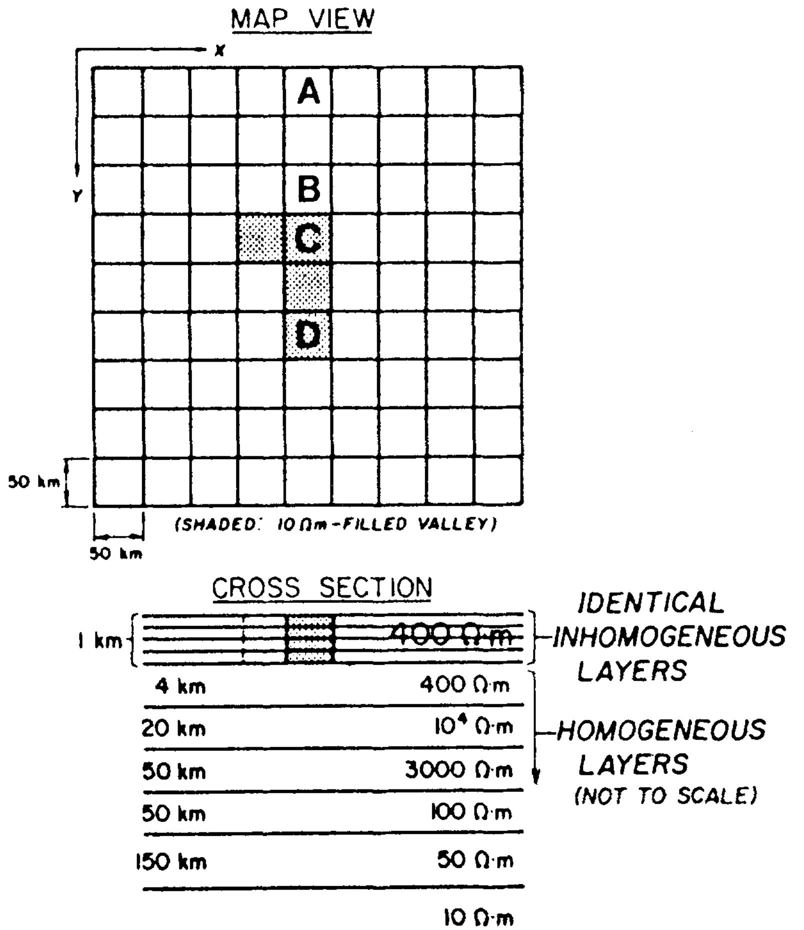

Fig. 21. Sketch of 3-D model geometry (taken from Park *et al.*, 1983).

Ranganayaki and Madden (1980) gave the adjustment distance, l_{ad} in their paper of generalized thin sheet approximation by

$$l_{ad} = \sqrt{(\sigma z_1)(\varrho z_2)} \tag{4}$$

where (σz_1) is the integrated conductivity of the upper part of the thin sheet and (ϱz_2) is the integrated resistivity of the resistive lower part of the thin sheet. They presented an adjustment distance of over 1000 km for the situation, where the ocean conductance is around 10–15 Sm^{-1} km and a resistivity thickness product of 10^5 Ωm km for the oceanic crust. Drury (1981) commented on this paper saying that the oceanic crustal resistivity values of 10^6 or 10^5 Ωm, which Ranganayaki and Madden (1980) used to calculate their large (over 1000 km) adjustment distance, were too high and he proposed an adjustment distance of approximately 140–150 km. In their reply Ranganayaki and Madden (1981) suggested oceanic telluric measurements specifically designed to determine the adjustment distance effect.

Dawson *et al.* (1982) made a numerical calculation for model parameters typifying an ocean-coast boundary underlain by a highly resistive crust. Their solution was analytical for H-polarization mode and they used also the generalized thin sheet (see Figure 13) and found that the residue of the pole associated with the resistive sheet dominates the solution for that example, the main consequence of which is a huge increase in the horizontal range over which the induced currents adjust themselves between the different skin-effect distributions at infinity on either side of the model. They concluded also that this adjustment distance has a more complicated dependence on the conductance and integrated resistivity of the sheet than what was proposed earlier by Ranganayaki and Madden (1980).

Vanyan (1981) considered distortion effects of a circular inhomogeneity of diameter L in a thin sedimentary cover. The ratio of total conductivities outside and inside the circle was equal to 10. The model included both the crustal and asthenospheric conductive layers on the normal background. His calculations for $L = 200$ and 1000 km with two different values of the uppermost crystalline rock resistivity 20000 and 2000 Ωm are presented in Figure 20. When $L = 1000$ km, the distortion is smaller, being almost absent for crystalline rock resistivity of 2000 Ωm. He presented the dimensionless distortion number, D, which is depending on the characteristic dimension L as follows $D = \sqrt{TS/L}$, where S is the total conductance of the sedimentary cover, and T is the resistivity x thickness product of the uppermost crystalline rocks. In his example the thickness was 10 km. His formula for D shows that local near-surface inhomogeneities with small characteristic dimension values of L can yield a fairly strong distortion to the MT field.

Thayer (1975) has presented an analytical solution of the electric field near a 2D offset in the earth's surface as a means of estimating the effects of nonplanar topography on telluric measurements. His results indicated that for an offset height d, the field at the earth's surface is within 10% of its undisturbed value for distances greater than 2.5 d from the offset on the lower side and for distances greater than 4 d on the upper side. The disturbance due to the offset extends even less far out in situations where the telluric currents are channeled close to the surface. These results are strictly true only for DC currents, but they hold approximately for two separate classes of situations: (i) time varying currents with skin depths in the channel which are much greater than the channel thickness, and (ii) offset heights, which are small with respect to both channel thickness and skin depth.

Park *et al.* (1983) considered effects of 3D structure on MT sounding curves. Their modeling program uses an extension of Ranganayaki and Madden's (1980) generalized thin sheet analysis. They used the model in Figure 21. Figure 22 depicts MT sounding for site B. The current gathering effect is seen at low frequencies. The effect is frequency-independent, when the thickness of the heterogeneous surface layer is much smaller than the EM skin depth. This effect is a parallel shift of the low-frequency 3D curve with respect to the 1D curve. This shift can be seen in Figure 22 for frequencies below 0.1 Hz. The skin depths inside and outside the heterogeneity at 0.1 Hz are 16 and 100 km, respectively. Current levels are perturbed from their

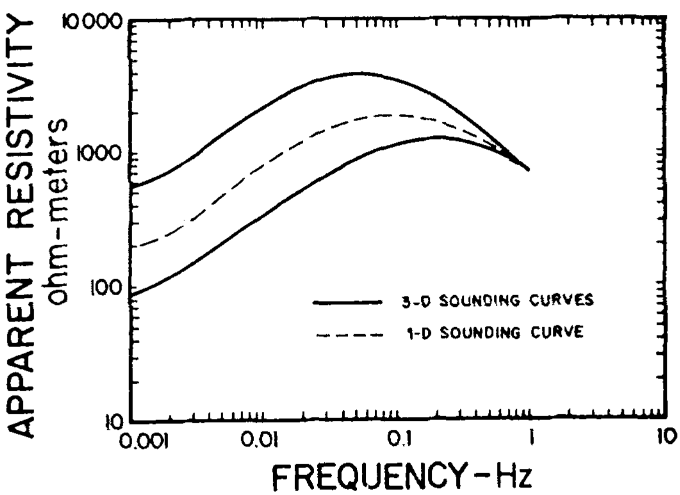

Fig. 22. 3-D model results – MT sounding for site B in Figure 21 (taken from Park *et al.*, 1983).

1D values near the boundary of a heterogeneity (see Figure 19). Excess current must be gathered by a conductor to raise the current level within the conductor to its 1D level. This excess current is gathered both horizontally and vertically. The horizontal distance over which a surface conductor gathers enough current vertically to decrease the current level perturbation by $1/e$ of its value at the boundary is the adjustment distance (Park *et al.*, 1983) (see the formula (4)). Park *et al.* (1983) compared the adjustment distance to the horizontal dimensions of the conductive feature to discriminate between horizontal and vertical current gathering. They found that if the dimensions are smaller than the adjustment distance, then most of the excess current present within the conductor has been gathered laterally. If the dimensions are much larger than the adjustment distance, then most of the excess current present has been gathered vertically. For example, for the model in Figure 21 the adjustment distance inside the heterogeneity is 187 km, and since the conductive valley is only 150 × 50 km so very little current has been gathered vertically. Most of the excess current that is present has thus been attracted laterally.

Jones (1983) proposed that a meaningful parameter to consider is the ratio of the strike length 1 to the skin depth in the host medium, i.e., $1/\delta_h$, when statements regarding the validity of approximating a 3D body by a 2D solution are being made. For an embedded body, the *H*-polarization results can be satisfactorily modelled by a 2D approach for rather small values of the parameter $1/\delta_h$. However, for the *E*-polarization $1/\delta_h$ must be at least unity for an adequate representation by a 2D model. Jones (1983) suggested a rough guide that the profile should be at least one δ_h away from either of the two faces. But we must remember the important meaning of the layering in the *E*-polarization case as was pointed out by Wannamaker *et al.* (1984a).

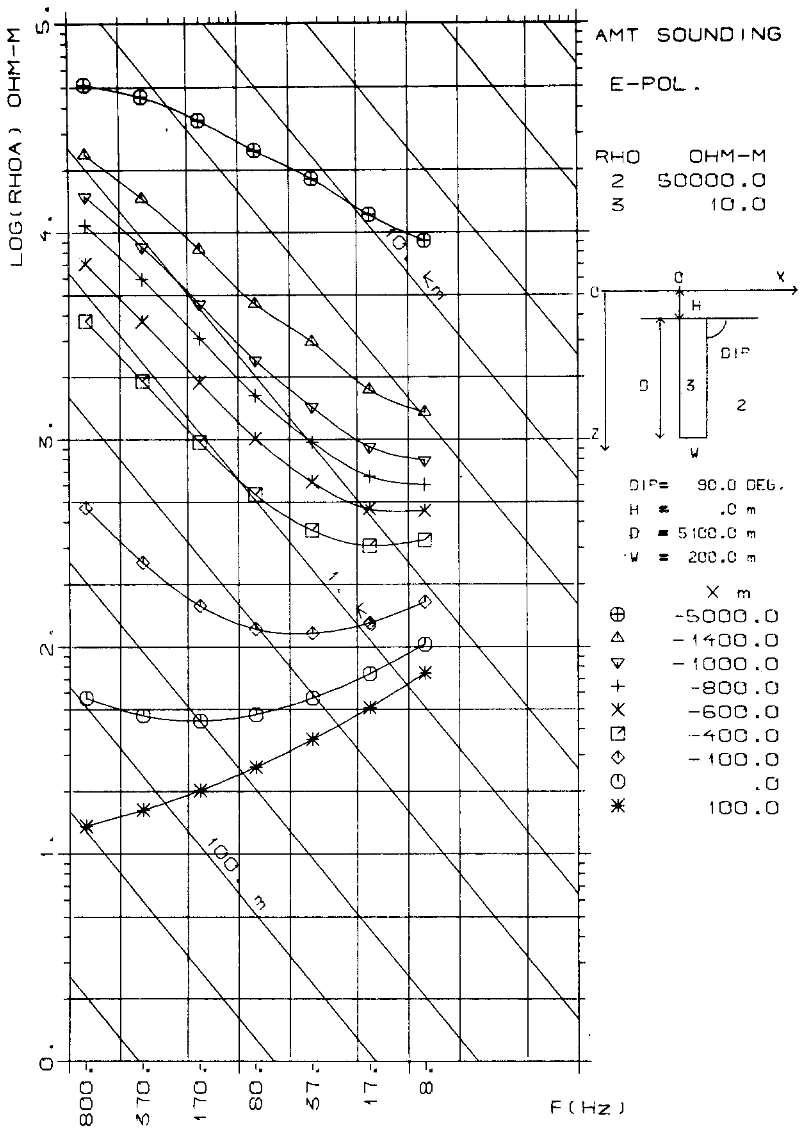

Fig. 23. The E-polarization AMT sounding curves by the finite element method for a vertical conducting dyke. Conductivity contrast is 5000 (taken from Kaikkonen, 1983).

That one δ_h, which Jones (1983) proposed, was approximately the distance from 2D vertical outcropping dyke where the induction effect still distorted E-polarization AMT sounding curves above 1D earth as Kaikkonen (1983) presented (Figure 23). As can be seen in Figure 23 the sounding curves indicate a false conducting layer at varying depths, which depend on the distance from the dyke and on the conductance of that.

Goldstein and Strangway (1975) and Sandberg and Hohmann (1982) have studied, when the plane-wave assumption is valid in using the controlled-source audiomagnetotellurics with a grounded electric dipole source. The former used an infinitesimal dipole source for their expressions for the magnetic and electric fields and concluded that if observations are made three or more δ_h away from the source, the conventional MT interpretations can be applied. The latter made their calculations for a finite length source and showed that for a half-space the plane-wave assumption is valid when the transmitter is more than 3 δ_h away in the broadside configuration and more than 5 δ_h away in the collinear configuration. 3D numerical modeling results for a dipole source 5 δ_h away compare well with those for a plane-wave source. In addition Sandberg and Hohmann (1982) found that depth of exploration was considerably less than a skin depth in conductive areas.

4. Conclusions

(1) Activity and progress in numerical EM modeling is distinctly concentrating in developing the algorithms which are capable of reducing the excessive computer storage and time needed by 3D solutions in general, or even 2D DE or hybrid solutions. This kind of work has been done by utilizing e.g., the group theory (Tripp, 1982; Tripp and Hohmann, 1984) and the summary representation (Raiche and Tarlowski, 1984; Tarlowski *et al.*, 1984).

(2) There is a great need of 2D and 3D TDEM numerical solutions.

(3) Similarly there is a need for approaches which are capable of taking care of regional and local effects by the same MT model.

(4) Some numerical 3D works have yielded valuable and new information (e.g., on 3D/2D relations) for interpretation of EM induction measurements (e.g., Park *et al.*, 1983; Wannamaker *et al.*, 1984a; Wannamaker *et al.*, 1984b).

(5) Progress in thin sheet approximations has been valuable and important in pointing out the role of distortions due to near-surface inhomogeneities and various characteristic dimensions (e.g., adjustment distance) (e.g., Dawson *et al.*, 1982). However, in this respect it is also necessary to do more calculations and analysing work.

(6) Importance and need of an everincreasing international co-operation (e.g., comparison of solutions and developing of programs, program library, research centre etc.) in numerical EM modeling is evident.

Acknowledgements

The reviewer wishes to thank all those who so kindly replied to his request to obtain information and material from their recent activity in the topic of this review paper.

References

Ádám, A.: 1981, 'Numerical Modeling Results', presented at the EM induction meeting of the Hungarian Geophysicists, Vezsprem, October 1981.

Ádám, A., Vanyan, L. L., Varlamov, D. A., Yegorov, I. V., Shilovski, A. P., and Shilovski, P. P.: 1982, 'Depth of Crustal Conducting Layer and Asthenosphere in the Pannonian Basin Determined by Magnetotellurics', *Phys. Earth Planet. Inter.* **28**, 251–260.

Brewitt–Taylor, C. R. and Weaver, J. T.: 1976, 'On the Finite Difference Solution of Two-Dimensional Induction Problems', *Geophys. J. R. Astr. Soc.* **47**, 375–396.

Červ, V., Pek, J., and Praus, O.: 1984, 'Models of Geoelectrical Anomalies in Czechoslovakia', *J. Geophys.* **55**, 161–168.

Coggon, J. H.: 1971, 'Electromagnetic and Electrical Modeling by the Finite Element Method', *Geophysics* **36**, 132–155.

Das, U. C. and Verma, S. K.: 1981, 'Numerical Considerations on Computing the EM Response of Three-Dimensional Inhomogeneities in a Layered Earth', *Geophys. J. R. Astr. Soc.* **66**, 733–740.

Das, U. C. and Verma, S. K.: 1982, 'Electromagnetic Response of an Arbitrarily Shaped Three-Dimensional Conductor in a Layered Earth-Numerical Results', *Geophys. J. R. Astr. Soc.* **68**, 55–66.

Dawson, T. W.: 1983, 'E-Polarization Induction in Two Thin Half-Sheets', *Geophys. J. R. Astr. Soc.* **73**, 83–107.

Dawson, T. W. and Weaver, J. T.: 1979a, 'Three-Dimensional Induction in a Non-Uniform Thin Sheet at the Surface of a Uniformly Conducting Earth', *Geophys. J. R. Astr. Soc.* **59**, 445–462.

Dawson, T. W. and Weaver, J. T.: 1979b, 'H-Polarization Induction in Two Thin Half-Sheets', *Geophys. J. R. Astr. Soc.* **56**, 419–438.

Dawson, T. W., Weaver, J. T., and Raval, U.: 1982, 'B-Polarization Induction in Two Generalized Thin Sheets at the Surface of a Conducting Half-Space', *Geophys. J. R. Astr. Soc.* **69**, 209–234.

d'Erceville, I. and Kunetz, G.: 1962, 'The Effect of a Fault on the Earth's Natural Electromagnetic Field', *Geophysics* **27**, 651–665.

Dmitriev, V. I. and Berdichevsky, M. N.: 1979, 'The Fundamental Model of Magnetotelluric Sounding', *Proceedings of the IEEE* **67**, 1034–1044.

Dosso, H. W.: 1966, 'Analogue Model Measurements for Electromagnetic Variations near Vertical Faults and Dykes', *Can. J. Earth Phys.* **3**, 287–303.

Dosso, H. W.: 1973, 'A Review of Analogue Model Studies of the Coast Effect', *Phys. Earth Planet. Inter.* **7**, 294–302.

Drury, M. J.: 1981, 'Comment on "Generalized Thin Sheet Analysis" by R. P. Ranganayaki and T. R. Madden', *Geophys. J. R. Astr. Soc.* **65**, 237–238.

Fainberg, E. B. and Zinger, B. Sh.: 1981, 'Electromagnetic Induction in a Spherical Model of the Earth with a Real Distribution of Near-Surface Conductivity', *Phys. Earth Planet. Inter.* **25**, 52–56.

Goldman, M. M. and Stoyer, C. H.: 1983, 'Finite-Difference Calculations of the Transient Field of an Axially Symmetric Earth for Vertical Magnetic Dipole Excitation', *Geophysics* **48**, 953–963.

Goldstein, M. A. and Strangway, D. W.: 1975, 'Audio-Frequency Magnetotellurics with a Grounded Electric Dipole Source, *Geophysics* **40**, 669–683.

Hermance, J. F.: 1978, 'Electromagnetic Induction in the Earth by Moving Ionospheric Current Systems', *Geophys. J. R. Astr. Soc.* **55**, 557–576.

Hermance, J. F.: 1982a, 'Refined Finite-Difference Simulations Using Local Integral Forms: Application to Telluric Fields in Two Dimensions', *Geophysics* **47**, 825–831.

Hermance, J. F.: 1982b, 'The Asymptotic Response of Three-Dimensional Basin Effects to Magnetotelluric Fields at Long Periods: The Effects of Current Channeling', *Geophysics* **47**, 1562–1573.

Hermance, J. F.: 1982c, 'Model Simulations of Possible Electromagnetic Induction Effects at MAGSAT Altitudes', *Geophys. Res. Lett.* **9**, 373–376.

Hermance, J. F.: 1983, 'DC Telluric Fields in Three Dimensions: A Refined Finite-Difference Simulation Using Local Integral Forms', *Geophysics* **48**, 331–340.

Hermance, J. F.: 1984, 'Electromagnetic Induction by Finite Wave-Number Source Fields in 2-D Lateral Heterogeneities; the Transverse Electric Mode', *Geophys. J. R. Astr. Soc.* **78**, 159–179.

Hohmann, G. W.: 1971, 'Electromagnetic Scattering by Conductors in the Earth Near a Line Source of Current', *Geophysics* **36**, 101–131.

Hohmann, G. W.: 1975, 'Three-Dimensional Induced Polarization and Electromagnetic Modeling', *Geophysics* **40**, 309–324.

Hohmann, G. W.: 1983, 'Three-Dimensional EM Modeling', *Geophysical Surveys* **6**, 27–53.

Hvoždara, M.: 1981a, 'Electromagnetic Induction of a Three-Dimensional Conductivity Inhomogeneity in the Two-Layered Earth, Part 1. Theory', *Studia geoph. et geod.* **25**, 167–180.

Hvoždara, M.: 1981b, 'Electromagnetic Induction of a Three-Dimensional Conductivity Inhomogeneity in the Two-Layered Earth, Part 2. Numerical Computations', *Studia geoph. et geod.* **25**, 393–403.

Jones, A. G.: 1983, 'The Problem of Current Channelling: A Critical Review', *Geophysical Surveys* **6**, 79–122.

Jones, F. W.: 1974, 'The Perturbation of Geomagnetic Fields by Two-Dimensional and Three-Dimensional Conductivity Inhomogeneities', *Pure and Appl. Geophys.* **112**, 793–800.

Jones, F. W. and Price, A. T.: 1970, 'The Perturbations of Alternating Geomagnetic Fields by Conductivity Anomalies', *Geophys. J. R. Astr. Soc.* **20**, 317–334.

Jones, F. W. and Pascoe, L. J.: 1971, 'A General Computer Program to Determine the Perturbation of Alternating Electric Currents in a Two-Dimensional model', *Geophys. J. R. Astr. Soc.* **23**, 3–30.

Jones, F. W. and Vozoff, K.: 1978, 'The Calculation of Magnetotelluric Quantities for Three-Dimensional Conductivity Inhomogeneities', *Geophysics* **43**, 1167–1175.

Jödicke, H., Untiedt, J., Olgemann, W., Schulte, L., and Wagenitz, V.: 1983, 'Electrical Conductivity Structure of the Crust and Upper Mantle Beneath the Rheinish Massif', in K. Fuchs *et al.* (eds.), *Plateau Uplift*, Springer-Verlag, Berlin, pp. 288–302.

Kaikkonen, P.: 1977, 'A Finite Element Program Package for Electromagnetic Modeling', *J. Geophys.* **43**, 179–192.

Kaikkonen, P.: 1980, 'Numerical Finite Element Modeling in Geophysical Applications of Electromagnetic Fields', Ph.D. thesis, Acta Univ. Oul. A 93, 1980. Phys. 18, 135 pp.

Kaikkonen, P.: 1983, 'Two-Dimensional Finite Element Modeling in Magnetotellurics', in S. E. Hjelt and L. L. Vanyan (eds.), *The Development of the Deep Geoelectric Model of the Baltic Shield*, Part 1. Numerical Methods, Dept. of Geophysics, Univ. of Oulu, Report No. 7, pp. 79–106.

Kaikkonen, P.: 1984, 'Some Results of the Thin Sheet Approximation for the Baltic Shield', in S. E. Hjelt (ed.), *The Development of the Deep Geoelectrical Model of the Baltic Shield*, Part 2. Proceedings of the 1st project symposium, Oulu, 15.–18.11.1983. Department of Geophysics, University of Oulu, Report No. 8, pp. 96–97.

Kaikkonen, P. and Pajunpää, K.: 1984, 'Audiomagnetotelluric Measurements across the Lake Ladoga-Bothnian Bay zone in Central Finland', *Geophys. J. R. Astr. Soc.* **78**, 439–452.

Kaikkonen, P., Vanyan, L. L., Okulessky, B. A., and Poray–Koshitz, A. M.: 1984, 'The Comparison of the Experimental MT Data with the Results of Numerical Modeling for the Kamchatka Peninsula', *Phys. Earth Planet. Inter.* **34**, 226–231.

Kaikkonen, P., Vanyan, L. L., Martanus, E. R., and Okulessky, B. A.: 1985, 'Contribution of the Surficial Effects on the Low-Frequency Magnetotelluric Anomaly at the Rheingraben Area', *Phys. Earth Planet. Inter.* **37**, 223–227.

Kaufmann, A. A.: 1978, 'Resolving Capabilities of the Inductive Methods of Electrroprospecting', *Geophysics* **43**, 1392–1398.

Ku, C. C., Hsieh, M. S., and Lim, S. E.: 1973, 'The Topographic Effect in Electromagnetic Fields', *Can. J. Earth Sci.* **10**, 645–656.

Kuo, J. T. and Cho, D.-H.: 1980, 'Transient Time-Domain Electromagnetics', *Geophysics* **45**, 271–291.

Lajoie, J. J. and West, G. F.: 1976, 'The Electromagnetic Response of a Conductive Inhomogeneity in a Layered Earth', *Geophysics* **41**, 1133–1156.

Lee, K. H., Pridmore, D. F., and Morrison, H. F.: 1981, 'A Hybrid Three-Dimensional Electromagnetic Modeling Scheme', *Geophysics* **46**, 796–805.

Madden, T. R. and Thompson, W.: 1965, 'Low Frequency Electromagnetic Oscillations of the Earth-Ionosphere Cavity', *Rev. Geophys.* **3**, 211–254.

Mareschal, M.: 1981, 'Source Effects and the Interpretation of Geomagnetic Sounding Data at Sub-Auroral Latitudes, *Geophys. J. R. Astr. Soc.* **67**, 125–136.

Mareschal, M. and Vasseur, G.: 1984, 'Bimodal Induction in Non-Uniform Thin Sheets: Do the Present Algorithms Work for Regional Studies?', *J. Geophys.* **55**, 203–213.

Mbipom, E. W. and Hutton, V. R. S.: 1983, 'Geoelectromagnetic Measurements Across the Moine Thrust and the Great Glen in Northern Scotland', *Geophys. J. R. Astr. Soc.* **74**, 507–524.

Menvielle, M., Rossignol, J. C., and Tarits, P.: 1982, 'The Coast Effect in Terms of Deviated Electric Currents: A Numerical Study', *Phys. Earth Planet. Inter.* **28**, 118–128.

Neves, A. S.: 1957, 'The Magneto-Telluric Method in Two-Dimensional Structures', Ph.D. thesis, Dept. of Geology and Geophysics, MIT, 186 pp.

Nienaber, W., Dosso, H. W., Law, L. K., Jones, F. M., and Ramaswamy, V.: 1979, 'An Analogue Model Study of Electromagnetic Induction in the Vancouver Island Region', *J. Geomagn. Geoelectr.* **31**, 115–132.

Osipova, I. L.: 1983, 'Consideration of the Influence of Ionospheric Source Field Structure on Deep Electromagnetic Sounding Results', in S. E. Hjelt and L. L. Vanyan (eds.), *The Development of the Deep Geoelectrical Model of the Baltic Shield*, Part 1. Numerical methods. Department of Geophysics, University of Oulu, Report No. 7, pp. 8–38.

Park, S. K., Orange, A. S., and Madden, T. R.: 1983, 'Effects of Three-Dimensional Structure on Magnetotelluric Sounding Curves', *Geophysics* **48**, 1402–1405.

Parry, J. R.: 1969, 'Integral Equation Formulations of Scattering from Two-Dimensional Inhomogeneities in a Conductive Earth', Ph.D. thesis, Univ. of California, Berkeley, 390 pp.

Praus, O.: 1976, 'Numerical Solutions of the MT Field in Inhomogeneous Structures', in A. Ádám (ed.), *Geoelectric and Geothermal Studies*, Akademiai Kiadó, Budapest, pp. 231–244.

Price, A. T.: 1949, 'The Induction of Electric Currents in Non-Uniform Thin Sheets and Shells', *Q. J. Mech. Appl. Math.* **2**, 283–310.

Price, A. T.: 1962, 'The Theory of Magnetotelluric Method When the Source Field is Considered', *J. Geophys. Res.* **67**, 1907–1918.

Price, A. T.: 1973, 'The Theory of Geomagnetic Induction', *Phys. Earth Planet. Inter.* **7**, 227–233.

Pridmore, D. F., Hohmann, G. W., Ward, S. H., and Sill, W. R.: 1981, 'An Investigation of Finite-Element Modeling for Electrical and Electromagnetic Data in Three Dimensions', *Geophysics* **46**, 1009–1024.

Raiche, A. P.: 1974, 'An Integral Equation Approach to Three-Dimensional Modelling', *Geophys. J. R. Astr. Soc.* **36**, 363–376.

Raiche, A. P. and Tarlowski, Z. K.: 1984, 'A Hybrid Method for Solving the Boundary Value Problems for Helmholtz's Equation in Two-Dimensional Domains', in J. Noye and C. Fletcher (eds.), *Computational Techniques and Applications: CTAC-83*, Proceedings of the 1983 International Conference on Computational Techniques and Applications held at the University of Sydney, Australia, North-Holland, Amsterdam, pp. 914–926.

Ranganayaki, R. P. and Madden, T. R.: 1980, 'Generalized Thin Sheet Analysis in Magnetotellurics: An Extension of Price's Analysis', *Geophys. J. R. Astr. Soc.* **60**, 445–457.

Ranganayaki, R. P. and Madden, T. R.: 1981, 'Reply to Comment on "Generalized Thin Sheet Analysis in Magnetotellurics: An Extension of Price's Analysis", by R. P. Ranganayaki and T. R. Madden' by Malcom J. Drury, *Geophys. J. R. Astr. Soc.* **65**, 239–240.

Rankin, D.: 1962, 'The Magnetotelleuric Effect of a Dike', *Geophysics* **27**, 666–676.

Rankin, D., Garland, G. D., and Vozoff, K.: 1965, 'An Analog Model for the Magnetotelluric Effect', *J. Geophys. Res.* **70**, 1939–1945.

Raval, U., Weaver, J. T., and Dawson, T. W.: 1981, 'The Ocean Coast-Effect Re-examined', *Geophys. J. R. Astr. Soc.* **67**, 115–123.

Reddy, I. K. and Rankin, D.: 1973, 'Magnetotelluric Response of a Two-Dimensional Sloping Contact by the Finite Element Method', *Pure and Appl. Geophys.* **105**, 847–857.

Reddy, I. K., Rankin, D., and Phillips, R. J.: 1977, 'Three-Dimensional Modeling in Magnetotelluric and Magnetic Variational Sounding', *Geophys. J. R. Astr. Soc.* **51**, 313–326.

Rijo, L.: 1977, 'Modeling of Electric and Electromagnetic Data', Ph.D. thesis, University of Utah.

Ritz, M.: 1983, 'The Distribution of Electric Conductivity on the Eastern Border of the West African Craton (Republic of Niger)', *Geophys. J. R. Astr. Soc.* **73**, 475–488.

Rodi, W. L.: 1976, 'A Technique for Improving the Accuracy of Finite Element Solutions for Magnetotelluric Data', *Geophys. J. R. Astr. Soc.* **44**, 483–506.

Sandberg, S. K. and Hohmann, G. W.: 1982, 'Controlled-Source Audiomagnetotellurics in Geothermal Exploration', *Geophysics* **47**, 100–116.

Scheen, W. L.: 1978, 'EMMMMA, a Computer Program for Three-Dimensional Modeling of Airborne Electromagnetic Surveys', Proc. of a workshop on modeling of electrical and electromagnetic methods, LBL-7053, 53–61.

Schmucker, U.: 1970, 'Anomalies of Geomagnetic Variations in the Southwestern United States', *Bull. Scripps Inst. Oceanography* **13**, 1–165.

Schmucker, U.: 1971, 'Interpretation of Induction Anomalies above Non-Uniform Surface Layers', *Geophysics* **36**, 156–165.

Schwarz, G.: 1984, 'Die elektrische Leitfähigkeit in der Toskana und ein daraus abgeleitetes geothermisches Modell – insbesondere für die Anomalie von Travale', Berliner geowiss. Abh., Berlin, Reihe B, Heft 8, 95S.

Silvester, P. and Haslam, C. R. S.: 1972, 'Magnetotelluric Modeling by the Finite Element Method', *Geophys. Prospecting* **20**, 872–891.

Spichak, V. V.: 1982, 'Electromagnetic Modelling over 3-D Structures', *Sixth Workshop on Electromagnetic Induction in the Earth and Moon*, Victoria, Canada, August 15–22, 1982, Abstract.

Stodt, J. A.: 1978, 'Documentation of a Finite Element Program for Solution of Geophysical Problems Governed by the Inhomogeneous 2-D Scalar Helmholtz Equation', NSF Program Listing and Documentation, University of Utah, 66 p.

Stoyer, C. H. and James, B. A.: 1983, 'The Time Domain Electromagnetic (TDEM) Method', Integrated Geosciences, Incorporated, 19 p.

Swift, C. M., Jr.: 1971, 'Theoretical Magnetotelluric and Turam Response from Two-Dimensional Inhomogeneities', *Geophysics* **36**, 38–52.

Tarlowski, C. Z., Raiche, A. P., and Nabighian, M.: 1984, 'The Use of Summary Representation for Electromagnetic Modeling', *Geophysics* **49**, 1506–1516.

Thayer, R. E.: 1975, 'Topographic Distortion of Telluric Currents: A Simple Calculation', *Geophysics* **40**, 91–95.

Ting, S. C. and Hohmann, G. W.: 1981, 'Integral Equation Modeling of Three-Dimensional Magnetotelluric Response', *Geophysics* **46**, 182–197.

Tripp, A. C.: 1982, 'Multidimensional Electromagnetic Modeling', Ph.D. Thesis, University of Utah, 179 p.

Tripp, A. C. and Hohmann, G. W.: 1984, 'Block Diagonalization of the Electromagnetic Impedance Matrix of a Symmetric Buried Body Using Group Theory', IEEE Transactions on Geoscience and Remote Sensing, GE-22, 62–69.

Vanyan, L. L.: 1981, 'Deep Geoelectrical Models: Geological and Electromagnetic Principles', *Phys. Earth Planet. Inter.* **25**, 273–279.

Varentsov, Iv. M.: 1983, 'Modern Trends in the Solution of Forward and Inverse 3D Electromagnetic Induction Problems', *Geophysical Surveys* **6**, 55–78.

Vasseur, G. and Weidelt, P.: 1977, 'Bimodal Electromagnetic Induction in Non-Uniform Thin Sheets with an Application to the Northern Pyrenian Induction Anomaly', *Geophys. J. R. Astr. Soc.* **51**, 669–690.

Wait, J. R.: 1954, 'On the Relation Between Telluric Currents and the Earth's Magnetic Field', *Geophysics* **19**, 281–289.

Wait, J. R.: 1962, *Electromagnetic Waves in Stratified Media*, Macmillan, New York, 372 pp.

Wannamaker, P. E., Hohmann, G. W., and SanFilipo, W. A.: 1984a, 'Electromagnetic Modeling of Three-Dimensional Bodies in Layered Earths Using Integral Equations', *Geophysics* **49**, 60–74.

Wannamaker, P. E., Hohmann, G. W., and Ward, S. H.: 1984b, 'Magnetotelluric Responses of Three-Dimensional Bodies in Layered Earths', *Geophysics* **49**, 1517–1533.

Ward, S. H.: 1967, 'Electromagnetic Theory for Geophysical Applications', in Mining Geophysics: Volume 2, Theory, SEG, Tulsa, pp. 10–196.

Weaver, J. T.: 1963, 'The Electromagnetic Field Within a Discontinuous Conductor with Reference to Geomagnetic Micropulsations near a Cost Line', *Can. J. Phys.* **41**, 484–495.

Weaver, J. T.: 1979, 'Electromagnetic Induction in Thin Sheet Conductivity Anomalies at the Surface of the Earth', *Proc. IEEE* **67**, 1044–1050.

Weaver, J. T.: 1982, 'Regional Induction in Scotland: An Example of Three-Dimensional Numerical Modelling Using the Thin Sheet Approximation', *Phys. Earth Planet. Inter.* **28**, 161–180.

Weaver, J. T. and Brewitt–Taylor, C. R.: 1978, 'Improved Boundary Conditions for the Numerical Solution of E-Polarization Problems in Geomagnetic Induction', *Geophys. J. R. Astr. Soc.* **54**, 309–317.

Weaver, J. T., Le Quang, B. V., and Fischer, G.: 1985, 'A Comparison of Analytic and Numerical Results for a Two-Dimensional Control Model in Electromagnetic Induction – I. B-Polarization Calculations', *Geophys. J. R. Astr. Soc.* **82**, 263–277.

Weidelt, P.: 1971, 'The Electromagnetic Induction in Two Thin Half-Sheets', *Z. Geophys.* **37**, 649–665.

Weidelt, P.: 1975, 'Electromagnetic Induction in Three-Dimensional Structures', *J. Geophys.* **41**, 85–109.

Weidelt, P.: 1977, 'Numerical Study of a Conductivity Channelling Effect', *Acta Geodaet., Geophys. et Montanist. Acad. Sci. Hung.* **12**, 195–205.

Yegorov, L. V., Chernyak, E. L., Palshin, N. A., Demidova, T. A., and Kaikkonen, P.: 1983a, 'Numerical Thin-Sheet Modelling of the Telluric Field Distortions by the Hybrid Technique. I. Theory and an Example for the Baltic Shield', *Phys. Earth Planet. Inter.* **33**, 56–63.

Yegorov, L. V., Chernyak, E. L., Palshin, N. A., Demidova, T. A., and Kaikkonen, P.: 1983b, 'Numerical Thin Sheet Modeling of the Telluric Field Distortions by the Hybrid Technique. II. Theoretical Background, an Example, the Computer Program, a Test Run and the Computer Listings', in S. E. Hjelt and L. L. Vanyan (eds.), *The Development of the Deep Geoelectric Model of the Baltic Shield*, Part 1. Numerical methods. Dept. of Geophysics, Univ. of Oulu, Report No. 7, pp. 39–78.

Zhdanov, M. S.: 1983, '*COMMEMI project*, Circular 1, Troitsk, 13 pp.

Zhdanov, M. S., Golubev, N. G., Spichak, V. V., and Varentsov, Iv. M.: 1982, 'The Construction of Effective Methods for Electromagnetic Modeling', *Geophys. J. R. Astr. Soc.* **68**, 589–607.